Advances in Water Resources 51 (2013) 104–122

Contents lists available at SciVerse ScienceDirect

Advances in Water Resources

journal homepage: www.elsevier.com/locate/advwatres

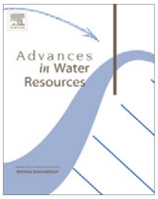

Nanoscale zero valent iron and bimetallic particles for contaminated site remediation

Denis O'Carroll [a,b,*], Brent Sleep [c], Magdalena Krol [a], Hardiljeet Boparai [a], Christopher Kocur [a]

[a] *Department of Civil and Environmental Engineering, The University of Western Ontario, 1151 Richmond Street, London, ON, Canada N6A 5B9*
[b] *Water Research Laboratory, School of Civil and Environmental Engineering, University of New South Wales, 110 King Street, Manly Vale, NSW, Australia*
[c] *Department of Civil Engineering, University of Toronto, 35 St. George Street, Toronto, ON, Canada M5S 1A4*

ARTICLE INFO

Article history:
Available online 23 February 2012

Keywords:
Nano zero valent iron (nZVI)
Colloid transport
Remediation
Bimetallic
Subsurface
Chlorinated solvents

ABSTRACT

Since the late 1990s, the use of nano zero valent iron (nZVI) for groundwater remediation has been investigated for its potential to reduce subsurface contaminants such as PCBs, chlorinated solvents, and heavy metals. nZVI shows tremendous promise in the environmental sector due to its high reactivity and as such, numerous laboratory and field studies have been performed to assess its effectiveness. This paper reviews the current knowledge of nZVI/bimetallic technology as it pertains to subsurface remediation of chlorinated solvents and heavy metals. The manuscript provides background on the technology, summarizing nZVI reactions with chlorinated solvents and metals, and examines the factors affecting nZVI reactivity. Studies on subsurface transport of bare and coated nZVI particles are also reviewed and challenges with field implementation are discussed. This manuscript offers a comprehensive review of nZVI technology and highlights the work still needed to optimize it for subsurface remediation.

1. Introduction

In the past, liquid wastes were disposed through direct pumping into the ground, migrated into the ground from leaky storage ponds and through surface spills, with no recognition of the likelihood that these wastes could persist in the subsurface for decades, potentially contaminating drinking water sources. Effluent slurries with high heavy metal content and non-aqueous phase liquids (NAPLs) are two common waste liquids that have been frequently disposed of improperly following a variety of industrial processes. Both heavy metals and chlorinated solvents, a particularly persistent NAPL contaminant, can contaminate water sources for decades and are one of the more common contaminants at brownfield and industrialized sites. Although a number of innovative remediation technologies have been developed, such as steam and density modified displacement, stabilization/solidification and *in situ* redox manipulation e.g. [1–4], existing technologies are rarely able to achieve clean up goals in contaminated aquifers at the completion of remedial activities. The problem relates to the inability of existing remedial technologies to remove, sequester or convert sufficient contaminant mass in the subsurface to significantly reduce aqueous phase concentrations and contaminant flux. The decisions related to site remediation are therefore still subject to considerable debate despite over two decades of active research and development [5,6]. The development of new and innovative remediation technologies is, therefore, crucial to achieve clean up goals at contaminated sites and ensure an abundant source of safe water for future generations.

The use of nanometals for subsurface remediation of chlorinated compound and heavy metal contaminated sites has received significant attention in part due to the ability of nanometals to rapidly transform contaminants in controlled laboratory experiments. Nanometals used for these purposes include nano iron and zinc, however nanoscale zero valent iron (nZVI) is most commonly used. In addition, other metals such as palladium or nickel have been added to increase the reduction rate. This combination of nZVI with a noble metal is referred to as a bimetallic nanometal. The reactivity and the availability of existing technology to precisely design and synthesize nanometals make nanometals particularly attractive for the remediation of subsurface contaminants. This remediation technology involves a series of steps for nanometals:

1. (1) transport, in the aqueous phase (or other delivery fluid), to the contaminated zone;
2. (2) attachment to soils in the contaminated zone or partitioning to the NAPL/aqueous phase;
3. (3) reaction with the target contaminant to form less toxic or less mobile products.

Nanometals have potential for use in remediation of a wide range of priority pollutants as indicated by a number of controlled

---

* Corresponding author at: Department of Civil and Environmental Engineering, The University of Western Ontario, 1151 Richmond Street, London, ON, Canada N6A 5B9.

E-mail address: docarroll@eng.uwo.ca (D. O'Carroll).

0309-1708/$ - see front matter © 2012 Elsevier Ltd. All rights reserved.
doi:10.1016/j.advwatres.2012.02.005

laboratory experiments e.g. [7–15]. However, further work is necessary to address the complexities associated with nanometal application at the field scale. For example, nanometals may react with various naturally occurring groundwater constituents decreasing the reducing equivalents available for reaction with the target contaminants. Another problem that has hampered the widespread implementation of nanometals is poor subsurface mobility. Due to strong attractive interparticle forces, primarily magnetic, nZVI, the typical nanometal used for remediation, tends to agglomerate to micron size particles, which have limited mobility in porous media. To overcome this problem, various polymers, and other coatings, have been used to stabilize nZVI particles, with varying degrees of success e.g. [16,17–24]. A number of field trials have been conducted to evaluate nZVI mobility and the impact of nZVI on chlorinated solvent contaminant mass and flux. However, several field scale applications have suffered from poor nZVI mobility [25,26]. Other studies have inferred good nZVI mobility but these mobility evaluations were based on measurements of contaminant reductions or total iron (i.e., including dissolved iron species) in wells downgradient of the injection well [27,28], rather than direct measurement of Fe^0 concentrations. Given these limited studies, additional work is required to assess field mobility and performance of nZVI/bimetallic nanometals at the field scale.

The goal of this review is to present the current state of knowledge related to the use of nZVI/bimetallic nanometals for the *in situ* remediation of chlorinated solvents and heavy metals. This work is divided into six main sections: nanometal reactivity with chlorinated compounds; reactivity with heavy metal target contaminants; factors affecting nZVI reactivity; nanometal mobility in controlled laboratory experiments; the current state of modeling nZVI subsurface transport; and outcomes of a series of nanometal field trials and lessons learned. Although nanometals have been used for the remediation of a variety of priority pollutants this work focuses on two classes (heavy metals and chlorinated solvents) that are of particular concern. Throughout this work, additional research needs and unresolved challenges are highlighted providing a comprehensive review as well as a look to the future of nZVI/bimetallic subsurface remediation.

2. Background

2.1. Development of zero valent metals for remediation

Although environmental nanotechnology for remediation applications was mainly developed in the last decade following the seminal work of Wang and Zhang [29], larger micron and millimeter size metals for contaminant destruction have been employed for some time. The first use of zero valent metals for degradation of chlorinated compounds in the environment was studied by Sweeney and Fischer [30] who used metallic zinc for the degradation of halogenated organic compounds. Subsequently, iron powder was used for the removal of chlorinated compounds from wastewater [31,32] as well as contaminated groundwater [33–35].

Gillham and O'Hannesin [34] were the first to show the effectiveness of zero valent iron (ZVI) for chlorinated ethane, ethene and methane degradation with normalized (to 1 m^2/ml) contaminant half-lives ranging from 0.013 to 20 h based on a series batch tests with ZVI. Matheson and Tratnyek [36] also reported rapid dehalogenation of carbon tetrachloride (CT) and chloroform using iron particles. In addition, ZVI was found to be effective for the remediation of a variety of priority pollutants, including metals [37–43], polychlorinated biphenyls (PCBs) [44,45], chlorinated pesticides [46–48], nitro aromatic compounds [49–51] and nitrates [52,53].

These studies, along with others [54–56], have resulted in application of ZVI, mostly in the form of permeable reactive barriers (PRBs) [33,38,57–61]. Although PRBs are effective at limiting off site migration of contaminants, they do not specifically target contaminant source zone remediation and have limited applications due to construction restrictions (i.e. depth of wall). Wang and Zhang [29] reported a method of synthesizing nanoscale ZVI (nZVI). This breakthrough was important for two reasons: the nZVI particles have a very high surface area to weight ratio, resulting in higher reactivity rates than micron scale ZVI when normalized to mass [12,29,35,62–64] and nZVI particles are smaller than most porous media pore throats. As a result, nZVI particles could theoretically be transported through the subsurface to a contaminant source zone. Since 1997, many studies have shown that nanometals are able to rapidly degrade a wide variety of priority pollutants e.g. [8,10,12–15,65]. Bimetallic nanoparticles and stabilizers have also been investigated and have been shown to enhance the reactivity and mobility of nanoparticles, respectively [11,16,21,27,66,67].

2.2. nZVI particle structure

Bare nZVI particles are typically less than 100 nm in diameter. In aqueous solutions, all nZVI particles react with water and oxygen to form an outer iron (hydr)oxide layer. As a result, nZVI particles have a core-shell structure [63,65,68] (Fig. 1). The thin and distorted oxide layer allows electron transfer from the metal (1) directly through defects such as pits or pinholes, (2) indirectly via the oxide conduction band, impurity or localized band, and (3) from sorbed or structural Fe^{2+}, thus sustaining the capacity of the particles for reduction of contaminants [62]. The outer (hydr)oxide layer may also act as an efficient adsorbent for various contaminants, including metals, as will be discussed in Section 4.

nZVI can be synthesized by a number of methods, including the sonochemical method, the electrochemical method, the gas phase reduction method, and the liquid phase reduction method [29,69–72]. Among these, gas phase reduction and liquid phase reduction are the most common methods for synthesizing nZVI for remediation purposes. nZVI particles synthesized by these methods rapidly develop a core-shell structure due to reaction with air or water, but may differ in particle size, surface area, degree of crystallinity, and thickness and composition of oxide shell [12,63,73]. Reactive nanoscale iron particles (RNIP), commercially

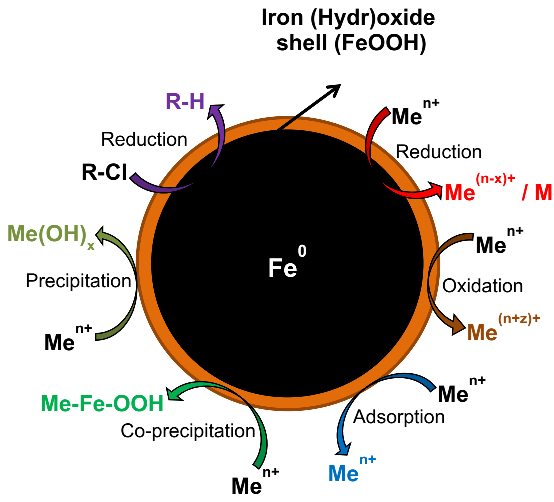

Fig. 1. Core–shell structure of nZVI depicting various mechanisms for the removal of metals and chlorinated compounds. Adapted from Li et al. [62].

available from Toda Kogyo Corp., are produced by reducing goethite and hematite particles at high temperatures with hydrogen gas [63,69]. These particles are made up of a relatively large α-Fe core and an outer magnetite (Fe_3O_4) shell [12,63,74], with reported particle diameters of 40–70 nm [12,63,74–76]. α-Fe can be defined as an allotropic form of pure iron having a body centered cubic (bcc) crystal structure [77]. Synthesizing nZVI using sodium borohydride (Fe^{BH}) results in amorphous particles with an α-Fe core and an outer shell consisting of iron (hydr)oxides [62,63,78]. These particles are typically 10–100 nm in diameter e.g. [12,15,29,63,75]. Although Wang and Zhang [29] identified a "periodic arrangement of iron atoms" using XRD analysis, which is indicative of crystal structures, Fe^{BH} nanoparticles have typically been characterized as amorphous [79]. This may be because even though Fe^{BH} particles have a crystalline core, the core diameters for Fe^{BH} are much smaller in size (<1.5 nm) than RNIP core diameters (30 nm) [63]. XRD studies also showed that Fe^{BH} cores were less ordered than RNIP cores [75]. These differences in nZVI structural properties strongly influence particle reactivity and the aging of particles, and therefore the particle efficiency (fraction of added Fe^0 in nZVI particles that is used in degrading contaminant) [12,63,75]. Liu et al. [75] examined the reductive dechlorination rates of Fe^{BH} when the Fe^0 core was poorly ordered/amorphous and the Fe^0 had been crystallized through annealing. The amorphous Fe^{BH} produced a greater reaction rate and extent of dechlorination of TCE with ethane as major end product when H_2 was externally supplied. In contrast, the rates of TCE dechlorination for the crystalline Fe^{BH} were similar in the presence and absence of externally supplied H_2. These results indicate that the amorphous Fe^0 in Fe^{BH} can catalyze the reaction of H_2 with chlorinated solvents, while the crystalline forms of Fe^0, such as in RNIP [12] would not have this catalytic effect. The crystallization of these particles resulted in less H_2 activation and slower TCE dechlorination, with acetylene as the major end product. Liu et al. [12] also found that Fe^{BH} efficiency was much higher than RNIP (92–52% respectively) with some inaccessible Fe^0 remaining in the RNIP particles but not in the Fe^{BH} particles. These studies show that the reactivity and efficiency of nanoparticles is dependent on particle characteristics and is an important consideration for remediation activities.

3. Reaction of chlorinated solvents with nanometals

As a strong reductant (i.e., reduction potential of −0.440 V [80]) iron reduces chlorinated compounds by reductive dehalogenation while being oxidized:

$$Fe^0 \xrightarrow{E^0=-0.44\ V} Fe^{2+} + 2e^- \tag{1}$$

Arnold and Roberts [54] and Li and Farrell [81] describe reductive dehalogenation via two reactive pathways: hydrogenolysis, and reductive elimination (dihaloelimination). Arnold and Roberts [54] note that reductive dehalogenation can occur via more than one pathway simultaneously in the same system.

Hydrogenolysis of chlorinated compounds, such as trichloroethene, involves replacement of a chlorine atom by a hydrogen atom and requires an electron donor as well as a proton donor (hydrogen) [82]. The general equation for reduction of chlorinated compounds by hydrogenolysis is [35,36]:

$$ClHC = CCl_2 + 2e^- + H^+ \rightarrow ClHC = CHCl + Cl^- \tag{2}$$

In reductive elimination (α or β), chlorine atoms are released by the chlorinated compound without addition of hydrogen. β-Elimination releases chlorine atoms, resulting in the decrease in the degree of saturation of the carbon–carbon bond. Eq. (3) is an example of β-elimination of a chlorinated ethene (such as TCE to chloroacetylene):

$$ClHC = CCl_2 + 2e^- \rightarrow HC \equiv CCl + 2Cl^- \tag{3}$$

β-Elimination can also occur with chlorinated ethanes, such as 1,2-DCA to vinyl chloride.

α-Elimination can also lead to dehalogenation of chlorinated compounds. This pathway is typically associated with compounds that have both chlorine atoms located on the same carbon and results in the formation of a carbene radical that can react rapidly to form ethene, avoiding the formation of vinyl chloride [54]:

$$Cl_2C = CH_2 + 2e^- \rightarrow H_2C = C: + 2Cl^- \tag{4}$$

Another reaction that is pertinent to systems undergoing reductive dechlorination is hydrogenation, which involves the addition of hydrogen across a double or triple carbon–carbon bond, converting alkynes to alkenes (acetylene to ethene for example) and alkenes to alkanes (ethene to ethane for example). This is often the last reaction after α or β-elimination and is often catalyzed with another metal or atomic hydrogen [12,36,83].

Iron can also react with water producing hydrogen gas [12,35]:

$$Fe^0 + 2H_2O \rightarrow Fe^{2+} + H_2 \uparrow + 2OH^- \tag{5}$$

This can lead to the formation of iron (hydr)oxide precipitates (e.g. $Fe(OH)_2$) resulting in the formation of a surface layer on nZVI particles [36,57,84].

Irrespective of the reductive pathway, electrons needed for reductive dehalogenation can be donated via three different mechanisms as described in Matheson and Tratnyek [36]. Direct oxidation of elemental iron at the metal surface transfers electrons to the reduced compound (Eq. (1)) and allows for dehalogenation of chlorinated compounds. The reduction of water (Eq. (5)) leads to the formation of hydrogen gas which can act as a reductant [12]. Dehalogenation with hydrogen as direct electron donor often requires a catalyst as H_2 alone is not a good reductant [36]. Fe^{2+} can also be oxidized to Fe^{3+} producing reducing equivalents for dehalogenation. This is a slow process and often requires the presence of ligands [36].

One significant concern of any remediation technology is the formation of daughter products that are more toxic than the parent compounds. Although hydrogenolysis can be an important dehalogenation pathway for many chlorinated solvents, the formation of vinyl chloride (VC) following the hydrogenolysis of PCE, TCE and cis-DCE is undesirable. In contrast, VC is not formed in the β-elimination of TCE [54]. However, Su and Puls [85] reported that TCE may be degraded by ZVI through both reaction pathways. Reductive dehalogenation studies with micro-sized ZVI suggest that the reduction of TCE and PCE using ZVI typically results in ethene and ethane with VC typically less than 10% of the daughter products [35,81], which may be an indication that β-elimination is the major pathway, or that any VC formed is rapidly degraded in the presence of ZVI. Arnold and Roberts [54] showed that β-elimination is much more common with chlorinated ethenes that possess α,β-pairs of chlorine atoms (e.g., TCE and PCE). Dehalogenation of chlorinated alkynes and carbon tetrachloride (CT) have been reported to follow hydrogenolysis [36,54]. Arnold and Roberts [54] propose that the reduction of 1,1-DCE to ethylene occurs via α-elimination (Eq. (4)), also avoiding the formation of VC.

These aforementioned studies investigating reductive dehalogenation pathways used micro-scale zero valent iron. Limited work has been completed examining the pathways associated with nZVI and the reductive degradation of chlorinated compounds although there is some evidence that the pathways are similar to the ones taken by larger ZVI particles. However, the pathway also seems to be dependent on the type of nanoparticle used [75,86], as well

Table 1
Standard redox potentials (E^0) in aqueous solution at 25 °C [80,219].

Aqueous solution	Half reactions	E^0 (V)
Chromium (Cr)	$CrO_4^{2-} + 8H^+ + 3e^- \leftrightarrow Cr^{3+} + 4H_2O$	1.51
Chromium (Cr)	$Cr_2O_7^{2-} + 14H^+ + 6e^- \leftrightarrow 2Cr^{3+} + 7H_2O$	1.36
Platinum (Pt)	$Pt^{2+} + 2e^- \leftrightarrow Pt$	1.19
Palladium(P)	$Pd^{2+} + 2e^- \leftrightarrow Pd$	0.92
Mercury (Hg)	$Hg^{2+} + 2e^- \leftrightarrow Hg$	0.86
Silver (Ag)	$Ag^+ + e^- \leftrightarrow Ag$	0.80
Arsenic (As^V)	$H_3AsO_4 + 2H^+ + 2e^- \leftrightarrow HAsO_2 + 4H_2O$	0.56
Copper (Cu)	$Cu^{2+} + 2e^- \leftrightarrow Cu$	0.34
Uranium (U)	$UO_2^{2+} + 4H^+ + 2e^- \leftrightarrow U^{4+} + 2H_2O$	0.27
Arsenic (As^{III})	$H_3AsO_3 + 3H^+ + 3e^- \leftrightarrow As + 3H_2O$	0.24
Copper (Cu)$^+$	$Cu^{2+} + e^- \leftrightarrow Cu^+$	0.16
Lead (Pb)	$Pb^{2+} + 2e^- \leftrightarrow Pb$	−0.13
Nickel (Ni)	$Ni^{2+} + 2e^- \leftrightarrow Ni$	−0.25
Cadmium (Cd)	$Cd^{2+} + 2e^- \leftrightarrow Cd$	−0.40
Iron (Fe)	$Fe^{2+} + 2e^- \leftrightarrow Fe$	−0.44
Zinc (Zn)	$Zn^{2+} + 2e^- \leftrightarrow Zn$	−0.76
Barium (Ba)	$Ba^{2+} + 2e^- \leftrightarrow Ba$	−2.92
1,2-Dichloroethane	$ClH_2C{-}CH_2Cl + 2e^- \leftrightarrow H_2C{=}CH_2 + 2Cl^-$	0.74
Carbon ttrachloride (CT)	$CCl_4 + H^+ + 2e^- \leftrightarrow CHCl_3 + Cl^-$	0.67
Tetrachloroethylene (PCE)	$Cl_2C{=}CCl_2 + H^+ + 2e^- \leftrightarrow Cl_2C{=}CHCl + Cl^-$	0.57
Trichloroethylene (TCE)	$Cl_2C{=}CHCl + H^+ + 2e^- \leftrightarrow Cl_2C{=}CH_2 + Cl^-$	0.53
Vinyl chloride (VC)	$ClHC{=}CH_2 + H^+ + 2e^- \leftrightarrow H_2C{=}CH_2 + Cl^-$	0.45
1,1-Dichloroethene (1,1-DCE)	$Cl_2C{=}CH_2 + H^+ + 2e^- \leftrightarrow ClHC{=}CH_2 + Cl^-$	0.42

as, the type of compound under investigation [15]. For example, similar to Arnold and Roberts [54], who used microscale ZVI, Song and Carraway [15] reported that chlorinated alkanes that possess α,β-pairs of chlorine atoms (i.e., each chlorine atom is on a different carbon atom such as hexachlorethane and perchloroethane) will undergo β-elimination when reduced by Fe^{BH}, while hydrogenolysis and α-elimination can both occur for compounds with all chlorine atoms on the same carbon (e.g., 1,1-DCA, 1,1,1-TCA). Liu et al. [12] compared the pathways for RNIP and Fe^{BH} nanoparticles under high and low TCE concentrations and found that the governing pathway was β-elimination for RNIP (as indicated by acetylene production) and primarily hydrogenolysis for Fe^{BH} particles. Reaction with Fe^{BH} also resulted in higher amounts of ethane than with RNIP. Only trace amounts of chlorinated by-products, such as cis-DCE and VC, were observed after reaction with both Fe^{BH} and RNIP in spite of the different dominant pathways. Fe^{BH} particles also increased dechlorination rates (higher k_{sa} – surface area normalized rate constant, L m^2/min) with both high and low TCE concentrations. Liu et al. [12] suggest that this is due to the catalysis of the reaction between TCE and H_2 that occurs with Fe^{BH}. Elsner et al. [86] also compared the reactivity of Fe^{BH} and RNIP with chlorinated ethenes using isotope analysis. Their conclusions are consistent with previous findings [12], that Fe^{BH} produced greater reaction rates than RNIP and that Fe^{BH} reduced chlorinated ethenes primarily through hydrogenolysis while RNIP reduced chlorinated ethenes primarily via β-elimination. Unlike microscale iron, where the compound plays a controlling factor in the pathway [54], nZVI studies suggest that pathways also depend on the form of zero valent iron in the particles.

Biodegradation of chlorinated ethenes (PCE and TCE) can also occur via hydrogenolysis. However, biodegradation of chlorinated ethenes can lead to production of substantial concentrations of VC. For example, *Dehalococcoides* (*Dhc*) strain 195 degrades VC cometabolically [87], leading to accumulation of VC in the biodegradation of PCE and TCE [88,89]. Isalou et al. [90] measured VC concentrations of 35.9 mg/L in columns with *Dhc* Strain 195 degrading 100 mg/L of PCE while Hood et al. [91] reported VC concentrations of approximately 60 mg/L after bioremediation activities at a TCE contaminated site. Other *Dhc* strains can biodegrade VC metabolically, and therefore produce lower peak VC concentrations. For example, Morrill et al. [92] used KB-1 (a mixed microbial culture that includes two strains of Dhc) in a bioaugmentation lab test and reduced TCE concentration to ethene, with final VC concentrations up to 8.9 mg/L. In studies of reductive degradation of TCE and PCE by nZVI, VC is consistently found only in trace amounts or non-detect [11,12,81], much lower than from biodegradation, likely due to the dominance of the β-elimination pathway with nZVI.

With nZVI injection the redox potential may be decreased substantially, leading to a potential increase in anaerobic microbial activity and biodegradation. In addition, microbes that dehalogenate chlorinated ethenes may use the H_2 produced from nZVI reaction with water. However, when Xiu et al. [93] examined the use of nZVI (RNIP) with a *Dhc* containing culture, they found that nZVI increased methanogenesis due to the production of H_2, and a temporary inhibition of TCE dechlorination was observed. The onset of accelerated TCE dechlorination and growth of dechlorinators was hypothesized to be due to passivation of nZVI. Xiu et al. [94] suggested that coating the nZVI particles with a copolymer could minimize the inhibitory effect on biodechlorination of chlorinated ethenes.

The addition of a second noble metal (e.g., Pd, Pt, Ni, Ag, or Cu) to the surface of nZVI particles yields bimetallic nanoparticles. Palladium is by far the most widely used metal for dehalogenation [95] and has been shown to act as a catalyst, greatly enhancing rates of reaction with nZVI e.g. [11,21,96,97–99]. Bimetallic nanoparticles are further discussed in Section 5.6.

4. Reaction of heavy metals with nanometals

Nanometals have been proposed for use in the remediation of a variety of contaminants, including heavy metals. The transformation, solubility, mobility, and consequently toxicity, of heavy metals in the environment are governed by redox reactions, precipitation/dissolution reactions, and adsorption/desorption phenomena. Water treatment strategies for removal of metal contaminants typically involve manipulating these mechanisms to control the availability and toxicity of metal contaminants to biota. The solubility, mobility and toxicity of metals of environmental concern are strongly dependent upon their oxidation states. For example, at its higher oxidation state chromium (Cr^{6+}) is very toxic, whereas Cr^{3+}, an essential nutrient, is relatively non-reactive but can be toxic in large doses. Moreover, Cr^{6+} is highly soluble and mobile in soils whereas Cr^{3+} forms relatively insoluble oxide and hydroxide compounds [100]. Given the strong dependence of Cr mobility and toxicity on its redox state, remediation technologies that reduce Cr^{6+}, such as a reduction by Fe^0, are of significant interest.

The specific removal mechanisms involved in treatment of heavy metal contamination with ZVI depend on the standard redox potential (E^0) of the metal contaminant (Table 1). Metals that have an E^0 that is more negative than, or similar to, that of Fe^0, (e.g., Cd and Zn) are removed purely by adsorption to the iron (hydr)oxide shell. Metals with E^0 much more positive than Fe^0 (e.g., Cr, As, Cu, U, and Se) are preferentially removed by reduction and precipitation [65]. Metals with slightly more positive E^0 than Fe^0, (e.g., Pb and Ni) can be removed by both reduction and adsorption. Oxidation and co-precipitation by iron oxides are the other possible reaction mechanisms depending upon the prevailing geochemical conditions such as pH, Eh and initial concentration and speciation of contaminant metals (Fig. 1). A group of metals (i.e., Pd, Pt, Ni, Cu) exhibiting catalytic properties, if present in oxidized forms in solution, can be reduced by nZVI to create bimetallic nanoparticles (Fe^0/M^0) enhancing the rate of reaction of contaminants (see Section 5.6). A variety of surface analysis techniques, including X-ray photoelectron spectroscopy (XPS), extended X-ray absorption spectroscopy (EXAFS), X-ray absorption near edge structure spectroscopy (XANES), X-ray diffraction (XRD) and scanning transmission electron microscopy (STEM) with energy dispersive X-ray (EDX), can be used to investigate the metal removal mechanisms associated with nZVI.

The metal-nZVI interactions for various metals can be categorized as:

1. Reduction – Cr, As, Cu, U, Pb, Ni, Se, Co, Pd, Pt, Hg, Ag.
2. Adsorption – Cr, As, U, Pb, Ni, Se, Co, Cd, Zn, Ba.
3. Oxidation/reoxidation – As, U, Se, Pb.
4. Co-precipitation – Cr, As, Ni, Se.
5. Precipitation – Cu, Pb, Cd, Co, Zn.

Some of the metals that can react with nZVI by more than one mechanism are reviewed here in detail.

Chromium (Cr) is a common pollutant at industrial waste sites and can be present in both trivalent (Cr^{3+}) and hexavalent (Cr^{6+}) states. The carcinogenic, soluble and mobile Cr^{6+} may be reduced to less toxic Cr^{3+} by nZVI and immobilized by precipitation as $Cr(OH)_3$ or by incorporation into the iron (hydr)oxide shell forming alloy-like Cr^{3+}–Fe^{3+} hydroxides [10,101,102]. Some Cr^{6+} will also directly adsorb on the hydr(oxide) shell of nZVI. These removal mechanisms have been confirmed by XPS, XANES and EXAFS analyses [10,101]. Relevant reactions between Cr and nZVI include [10]:

(A) Reduction of Cr^{6+} to Cr^{3+}:

$$3Fe^0 + Cr_2O_7^{2-} + 7H_2O \rightarrow 3Fe^{2+} + 2Cr(OH)_3 + 8OH^- \quad (6)$$

(B) Formation of mixed Cr^{3+}–Fe^{3+} hydroxides:

$$xCr^{3+} + (1-x)Fe^{3+} + 3H_2O \rightarrow Cr_xFe_{1-x}(OH)_3 + 3H^+ \quad (7)$$

$$xCr^{3+} + (1-x)Fe^{3+} + 2H_2O \rightarrow Cr_xFe_{(1-x)}OOH + 3H^+ \quad (8)$$

The Cr to Fe atomic ratio in mixed Cr^{3+}–Fe^{3+} hydroxides varies depending on the reaction conditions including pH and Cr^{6+} concentration.

(C) Adsorption of Cr^{6+}:

$$\equiv FeOH + Cr_2O_7^{2-} \rightarrow \equiv Fe - Cr_2O_7^- + OH^- \quad (9)$$

The formation of mixed Cr^{3+}–Fe^{3+} hydroxides on the oxidized nZVI surface layer may inhibit further electron transfer from the Fe^0 core to Cr^{6+} at later reaction times, favoring adsorption of Cr^{6+} on the nZVI surface, especially at high Cr^{VI} concentrations [10,103]. This self-inhibition of the reduction reaction can be overcome using bimetallic nanoparticles (e.g., Cu^0/Fe^0 and Pd^0/Fe^0) to increase both the rate and extent of Cr^{6+} removal by reductive precipitation [103,104]. Though these short-term studies demonstrate an effective removal of Cr^{6+} by nZVI via reductive precipitation and co-precipitation, additional research is needed to further explore the overall efficiency of nZVI for remediation of Cr^{6+} contaminated groundwater where the prevailing geochemical conditions can influence these removal mechanisms.

Arsenic (As), a confirmed carcinogen, is present as arsenate (As^{5+}) and arsenite (As^{3+}) in groundwater throughout the world. As^{3+} is much more toxic and generally more mobile than As^{5+} [105]. As^{5+} can be reduced by nZVI to either As^0 or As^{3+} as confirmed by the XPS analysis [106]. Any remaining As^{5+} is adsorbed onto iron oxides in the outer layer of the iron nanoparticles [106,107]. As^{3+}, thus formed, is either adsorbed or co-precipitated at the iron nanoparticle surface [106,108]. Some As^{3+} is also reported to be oxidized to As^{5+} either by hydroxyl radicals or by iron oxides (both formed during oxidation of Fe^0) via formation of iron oxide-As^{3+} surface complexes [106,108,109]. Adsorption of both As^{3+} and As^{5+} on iron nanoparticles occurs by forming inner-sphere complexes with the (hydr)oxide shell of nZVI [109–111].

While studying the removal of As^{3+} by nZVI, 51% of the total As^{3+} was found as surface bound As^{3+} whereas 14 and 35% was transformed to As^{5+} by iron oxides and As^0 by Fe^0 respectively, indicating that nZVI exhibits broad functionality with the Fe^0 core having reduction capability and the (hydr)oxide layer promoting oxidation and adsorption/co-precipitation [106,108]. These studies suggest that under most common geochemical conditions there will be a mechanism by which application of nZVI will lead to treatment of As, leading to a potential for development of a robust nZVI *in situ* treatment technology for subsurface As contamination.

Uranium (U) is the most common radionuclide contaminant found at many nuclear waste sites. It is mainly detected in contaminated groundwater as highly soluble and mobile U^{6+} [112] and can be remediated by reducing it to insoluble U^{4+} oxides by various reductants [113]. Reduction of U^{6+} to U^{4+} by ZVI is thermodynamically favorable [114]. U^{6+} will be predominantly removed by nZVI via reductive precipitation of UO_2 (U^{4+}) with minor precipitation of $UO_3{\cdot}2H_2O$ (U^{6+}) as confirmed by the XPS and XRD analyses [113,115–117]. U^{4+} may slowly reoxidize and redissolve as U^{6+} with concurrent reduction of Fe^{3+} to Fe^{2+}. The reoxidized U^{VI} may be removed via sorption onto the surfaces of iron (hydr)oxides [116]. This suggests that the formation of iron hydr(oxides) during oxidation of Fe^0 also plays an important role in removing U especially after reoxidation of U^{4+}.

Selenium enters the environment naturally from weathering of minerals and anthropogenically from mining, agricultural, petrochemical and industrial operations. The toxicity and solubility of Se depends on the redox conditions. The formation of soluble selenate (SeO_4^{2-} or Se^{6+}) and selenite (SeO_3^{2-} or Se^{4+}) is favored under oxidizing conditions, and formation of insoluble elemental Se (Se^0) and selenide (Se^{2-}) is favored under reducing conditions [118]. The reduction of Se^{6+} to Se^{2-} can be written as [80]:

$$SeO_4^{2-} \overset{E^0=0.03}{\rightarrow} SeO_3^{2-} \overset{-0.36}{\rightarrow} Se \overset{-0.67}{\rightarrow} Se^{2-} \quad (10)$$

The reduction of soluble Se^{6+} to insoluble Se^0 by nZVI is thermodynamically favorable, but further reduction to Se^{2-} is not. Se^{6+} removal is quite complex with a variety of removal mechanisms possible (e.g., reduction, complex formation, adsorption and reoxidation). These removal mechanisms have been shown to occur through investigation by SEM-EDX, XANES and EXAFS [119,120]. For example, Se^{6+} can be reduced to Se^{2-} via formation of Se^{4+} and Se^0 which can then either complex with Fe^0 oxidation products forming iron selenide (FeSe) or reoxidize to Se^0 and Se^{4+}. The Se^{4+} can be immobilized by strongly binding to iron (hydr)oxides via inner-sphere adsorption [120]. This indicates that nZVI is capable of removing various Se species even after oxidizing to iron hydr(oxides). More research is needed to investigate the long term stability of various Se species formed after interaction with nZVI as these can be impacted by groundwater chemistry.

Nickel (Ni^{2+}) and lead (Pb^{2+}), common pollutants of electroplating industry, may be removed by nZVI via reduction to Ni^0 and Pb^0 and by adsorption as Ni^{2+} and Pb^{2+} [65,102,121–123]. While reacting with nZVI, Pb^{2+} also precipitates as $Pb(OH)_2$ and oxidizes as α-PbO_2 as confirmed by the XRD analysis [102,124]. Detailed XPS analysis shows that Ni^{2+} is initially bound to the nZVI surface by physical sorption, then binds strongly by chemisorption and finally reduced to Ni^0 as described here [122]:

$$\equiv FeOH + Ni^{2+} \rightarrow \equiv FeO{-}Ni^+ + H^+ \quad (11)$$

$$\equiv FeONi^+ + H_2O \rightarrow \equiv FeONi{-}OH + H^+ \quad (12)$$

$$\equiv FeONi^+ + Fe^0 + H^+ \rightarrow \equiv FeOH - Ni + Fe^{2+} \quad (13)$$

Other metals of environmental importance, including Cu^{2+}, Hg^{2+} and Ag^{2+} may be sequestered via chemical reduction to their elemental forms [9,65,78,124,125]. Cu^{2+} may also be reduced to Cu^{+} by nZVI resulting in the formation of Cu_2O [9,124]. However, the sorption of these metals on the oxidized nZVI surface prior to their reduction cannot be ignored as the (hydr)oxide layer on the nZVI surface has high sorption affinity for metal cations [65,78]. Metals with E^0 more negative or close to that of Fe^0 (e.g., Co, Cd, Zn and Ba) will be removed by sorption and/or precipitation [7,65,78,125–127]. The addition of nZVI to aqueous systems usually increases the pH to 8.0–8.2 due to generation of OH^- from reduction of water by Fe^0, resulting in the immobilization of metals by precipitation as hydroxides. Zn and Co may also be removed by precipitation on the oxidized nZVI surface as $Zn(OH)_2$ and $Co(OH)_2$ [78,126]. These studies suggest that other metal contaminants with more negative redox potentials than Fe^0 (e.g., Be, Ra, Th, Pu, Sr, Mn, Cs) may be removed by adsorption and precipitation on the nZVI surface.

Metal catalysts (e.g. Pd, Pt, Ni, and Cu) with E^0 more positive than Fe^0 may be reduced by nZVI to form bimetallic iron nanoparticles (Fe^0/Pd^0, Fe^0/Pt^0, Fe^0/Ni^0 and Fe^0/Cu^0). A small amount of metal catalyst deposited on the nZVI surface increases contaminant transformation rates significantly [67,103,124]. These metal catalysts, existing as co-contaminants at mixed waste sites, can be manipulated to form *in situ* bimetallic iron nanoparticles, enhancing the remediation process [124]. For example, Cr^{6+} removal is significantly enhanced using bimetals (e.g., Fe^0/Cu^0, Fe^0/Pd^0 and Fe^0/Ni^0) [103,104,128]. Bimetallic iron nanoparticles play an important role in overcoming the self-inhibition of metal removal reactions by preventing oxide formation on the nZVI surface. More research using bimetals is needed for the metals like U and Se, which get reoxidized or redissolved at later times of reaction with nZVI.

A large number of metals can be removed by adsorption. As such a detailed understanding of adsorption kinetics and thermodynamics is important to design for the optimal pathway (e.g., chemisorption versus physisorption) and sorption mechanism (e.g. surface versus intraparticle diffusion) to maximize adsorption rates and adsorptive capacity of nZVI for specific metals. Few studies have investigated adsorption kinetics and thermodynamics of metal removal by nZVI [7,107,109,127,129,130]. Arsenic (As^{3+} and As^{5+}) adsorption exhibited a pseudo-first-order rate and could be fitted well with both Freundlich and Langmuir isotherm models [107,109]. The kinetics and thermodynamics of cadmium adsorption on nZVI provide evidence that Cd removal by nZVI occurs via chemisorption with surface diffusion as the rate-limiting step [7]. More research is needed to investigate adsorption mechanisms, kinetics, and thermodynamics for other metals that may be removed by adsorption to nZVI particles.

5. Factors affecting reactivity of nZVI with metals and chlorinated solvents

As shown by several studies, there are many factors impacting nZVI reactivity with chlorinated compounds and metals. In addition to the degree of crystallinity of the Fe^0 core, which was discussed in Section 2, factors affecting nZVI reactivity include surface area [15,63,104,107,131], age of the nanoparticle [79,132,133], aqueous phase pH [15,36,79,81,107,119,134,135], nZVI stabilizers [16,18,21,76,136], and concentrations of contaminants and other reactive groundwater constituents [12,15,137,138]. These effects will be discussed in greater detail in the following sections.

5.1. Surface area

Gillham and O'Hannesin [34] were the first to report that greater ZVI surface area resulted in greater rates of dehalogenation of chlorinated compounds. This helped spur interest in nano-scale ZVI, since smaller particles have a much higher surface area to mass ratio. For example, nZVI surface area can be in excess of 40 m^2/g for stabilized particles [16,21,139] and 15–34 m^2/g for bare particles, with Fe^{BH} having greater surface area than RNIP particles, e.g. [29, 63, 136, 139]. Catalyst metals like Ni have been reported to further increase the surface area of bimetallic particles (Fe^0/Ni^0) when they are added to the iron precursor prior to the borohydride reduction step [67,140]. Micron scale ZVI has a surface area on the order of <1 m^2/g [29,36,63]. Nurmi et al. [63] showed that nanoparticles (both RNIP and Fe^{BH}) exhibited greater reactivity than micro-sized iron particles for reduction of CT on a per mass basis. However, when normalized to surface area the rate constants were similar for both nano and micro-sized particles suggesting that a nano-effect may not exist. The presence of a larger number of reactive sites on nZVI particles, as compared to mZVI particles may enhance nZVI reactivity [63,131]. The larger surface area of nZVI than mZVI also provides greater density of reactive sites for reduction and adsorption of metals thus increasing the removal rate and capacity of nZVI. Kanel et al. [107] found the k_{sa} (surface area normalized rate constant, L m^2/min) of arsenic removal by nZVI to be 1-3 orders of magnitude larger than that of microscale ZVI. Similarly, Rivero-Huguet and Marshall [64] reported enhanced removal of Cr^{6+} by nano iron due to the increased specific surface area and higher surface reactivity of the nano iron. Since nanoparticles tend to aggregate (due to magnetic and van der Waals forces), it is unclear whether the reactivity of nZVI will change due to the decrease in surface area/unit mass or remain unchanged from the original reactivity of the individual nanoparticles [63,131].

5.2. Aging

nZVI rapidly oxidizes in aqueous solutions by reacting with oxygen or water or through reaction with naturally occurring subsurface constituents. When nZVI is exposed to water several processes can occur. The original oxide shell can break down due to reaction with water [141] or autoreduction (reduction of the oxide shell by underlying Fe^0), allowing for the freshly formed Fe^0 to oxidize, coupled with the reduction of electron acceptors in the water. In addition, the particles can aggregate and a new, mixed-valence (Fe^{2+}–Fe^{3+}) oxide layer can form [132]. nZVI aging/oxidation results in a loss of Fe^0 content [12,79,132], decreasing the reducing equivalents available for reaction with the target contaminant. Due to the time elapsed between nZVI synthesis and nZVI arrival at the target source zone, this loss should be accounted for in determining the required amount of nZVI for contaminant transformation. At present there is limited ability to predict the additional nZVI requirements to account for the loss of Fe^0 content in various subsurface environments.

A number of studies have investigated the impact of aging on nZVI reactivity. Sarathy et al. [132] reported a decrease in Fe^0 content after exposing RNIP to water for six months. They observed an initial (2 day) increase in the CT mass-normalized, first-order, degradation rate constant (k_M) followed by a gradual decrease in k_M. Kim et al. [142] observed a similar trend for TCE degradation rates, using shell-modified RNIP exposed to air or water. This change in rate constants with aging was attributed to depassivation of particles initially followed by repassivation upon prolonged exposure [132,142]. Wang et al. [143] also reported decrease in reactivity of Fe^{BH} that was stabilized with inert gas and then exposed to air.

Liu and Lowry [79] also studied reactivity changes with aging of RNIP. Although they observed a significant initial decrease (for the first 10 days) in TCE reaction rate constants, the TCE reaction rate remained nearly the same or increased slightly for the rest of the study period. They reported nearly the same reaction rate constants (at day 20), irrespective of the Fe^0 content, and concluded that the TCE reaction is zero-order with respect to the Fe^0 content of RNIP. Similarly, Liu et al. [75] reported that the partial oxidation of Fe^{BH} particles did not significantly affect the maximum Fe^0-normalized reaction rate of TCE or the reaction product distribution, although partially oxidized particles were reported to have longer periods of lower reactivity when compared to fresh Fe^{BH} particles.

Differences in results in these various studies might be due to differences in reaction conditions such as pH, initial contaminant concentration, method of nZVI synthesis/stabilization, exposure time, and medium for oxidation (air or water). For example, aging of shell-modified RNIP in water resulted in formation of a goethite surface layer whereas exposure to air yielded wüstite, hematite and maghemite surface layers in addition to pre-existing magnetite [142]. Although the thickness of the oxide layer is reported to be constant with aging, the composition may change [132,144]. Any changes to the iron oxide surface characteristics could affect reactivity, as adsorbed Fe^{2+} is capable of mediating reductive transformation of chlorinated solvents and metal contaminants [145–147].

Catalysts are commonly used to increase reaction rates by decreasing the activation energy; however they can also affect the aging process and consequently the reactivity of bimetallic nZVI particles. Yan et al. [148] deposited Pd^0 on the surface of fresh nZVI particles. After aging for 24 h no Pd was detected on the nZVI surface, indicating that it may have become embedded under the oxide shell. No metallic iron was detected by XPS suggesting that particles had undergone severe oxidation upon aging. Reactivity of the Pd-nZVI with TCE, aged in water for 24 h, decreased by 80% compared to that of the fresh Pd-nZVI particles. Similar results were found by Zhu and Lim [99] for aged Pd-nZVI (in water for 24 h) and 1,2,4-trichlorobenzene. This decrease was attributed to detachment of Pd from iron and its encapsulation in iron oxides formed during nZVI oxidation. These studies suggest that the decreased reactivity of aged bimetallic nanoparticles is due to their oxidation and is similar to uncatalyzed nZVI.

nZVI oxidation can also have a significant impact on heavy metal removal rates and mechanisms. The reduction of metals by nZVI can be slowed or inhibited due to the oxidation of nZVI particles. Metals (e.g., U and Se) that are initially reduced by Fe^0 can be partly reoxidized with reduction of iron oxides in the iron nanoparticles [116,120]. As most metal contaminants can be removed by adsorption at the iron oxide surface, adsorption may become the dominant removal mechanism after oxidation of nZVI particles. Although nZVI aging has been identified as a significant issue impacting reactivity, limited work has been has been completed in this area and more research is needed.

5.3. pH

pH strongly influences the redox reactions occurring at the ZVI surface by accelerating corrosion at low pH (Eq. (1)) and passivating the iron surface at high pH through the formation of iron hydr(oxides) [15,36].

The oxidation of Fe^0 in aqueous systems releases OH^- ions, increasing the pH of the system (>8.0) as shown in Eq. (5) and in the following reaction:

$$2Fe^0 + O_2 + 2H_2O \rightarrow 2Fe^{2+} + 4OH^- \qquad (14)$$

Given these reactions, the high iron mass ratio (10–50 wt%) (i.e., ratio of iron mass to iron plus water mass in a given volume) of micro and granular iron used in PRBs can buffer groundwater pH at 8–9 resulting in iron passivation [79]. However, the iron mass ratio of nZVI in injection suspensions is much lower (0.2–0.5 wt%), favoring corrosion at a prevailing near neutral pH. Thus, iron longevity/efficiency can differ for micro- and nano-iron particles under the same field conditions.

A number of studies have reported an increase in reaction rates with decreasing pH for reductive dehalogenation of chlorinated compounds by RNIP and Fe^{BH} [15,79,149–151]. This may be attributed to greater availability of electrons from the Fe^0 core due to dissolution of the oxide layer at low pH. pH not only affects reaction rates but also the dominant reaction pathways.

Liu and Lowry [79] studied the effect of pH on H_2 evolution rates (k_{H_2}) of RNIP. Decreasing the pH resulted in an increased k_{H_2} and TCE reaction rates (k_{obs}), and the increase in k_{H_2} was an order of magnitude greater than k_{obs} over the same pH range. A fitted linear relationship between pH and k_{obs} had a weak dependence, indicating that TCE dechlorination does not strongly depend on pH. H_2 evolution had little effect on TCE dechlorination rates by RNIP, while Liu et al. [75] showed that addition of H_2 to systems with Fe^{BH} resulted in higher rates of dechlorination. Evolution of H_2 can also positively impact microbial degradation of contaminants [152]. In this case, addition of nZVI to the subsurface may have prolonged remediation benefits if microbial dechlorination is stimulated.

Outer ZVI shell characteristics [135,153] may be affected by pH. The extent to which pH affects the formation of the oxide layer at the nanoscale ZVI surface is not fully understood. Liu and Lowry [79] suggest that different Fe-oxides phases may exist on RNIP particles at different pH while Song and Carraway [15] propose that Fe^{BH} is less passivated than microscale ZVI as they observed a smaller effect of pH on the reaction rate constant for nanoscale nZVI than microscale ZVI [36].

The impact of pH on metal removal by nZVI depends on the oxidation state of the metal and the removal mechanism. Passivation of the nZVI surface at high pH hinders electron transfer from the Fe^0 core, thus, decreasing the removal of metal contaminants by reductive precipitation. For example, Se^{VI} removal by nZVI decreased from 91% to 11% with increase in pH from 3.5 to 11 [119]. High pH also decreases adsorption of metal anions due to electrostatic repulsion caused by the negative nZVI surface charge above the pH of 7.8 [107,109]. However, this negatively charged nZVI surface is favorable for adsorption of metal cations. Some metals are immobilized via precipitation by hydrolyzing as metal hydroxides at high pH (e.g., Cd, Zn, Co, Cu). More research is needed to study the effect of pH on metal removal by nZVI to determine the specific impact on each removal mechanism.

5.4. Coatings/stabilizers

Numerous reports have shown that nZVI particles quickly aggregate, decreasing surface area for reaction and limiting mobility (see Section 6.1). Therefore, different coatings/stabilizers have been used to stabilize nanoparticles in the subsurface [e.g., 16,21–23,154, 155–158] providing higher surface area for reaction [157]. These coatings include guar gum, carboxylmethyl cellulose (CMC), poly-styrene-sulfonate (PSS) and poly(methyl)methacryl and can be applied by: (1) physically absorbing polymer coatings on existing nZVI particles in a post-synthesis process, e.g. [22,159,160]; (2) synthesizing nZVI in the presence of polymer which concurrently stabilizes the particles, e.g. [16,17,23]. There are also emerging techniques to synthesize nanoparticles that incorporate ZVI into a matrix [24,155,156,161,162] or membrane [163].

It is important to distinguish between the methods of coating nZVI with polymer as the different processes affect particle structure (see Section 2.2), as well as colloidal stability (see Section 6.2). Literature studies have reported conflicting reactivity results that likely depend on the stabilization approach and the type of stabilizer. The post-synthesis stabilization approach has been shown to decrease reactivity [136] whereas the pre-synthesis approach has improved reactivity and significantly increased surface area [16]. In the case of the post-synthesis process, decreased reactivity has been attributed to a number of mechanisms, including reaction sites on the surface of nZVI being blocked by the polymer, the diffusion of aqueous phase contaminant to the surface being inhibited. The slow diffusion of reaction products away from the surface may inhibit desorption from reactive sites [136]. The dominant process will depend on the concentration of the polymer on the surface [136] and may differ depending on the properties of the polymer coating. Wang et al. [139] showed that there is competition for contaminant between the reactive sites on the nZVI and sorption sites on the polymer coating. However, the loss of reactivity was not significant and must be weighed against benefits provided by the polymer coating. In addition, it has been suggested that several polymer coatings are readily available for biological degradation [18,164], and in some cases natural polymers (i.e., humic and fulvic acids) can act as a co-reactants or electron donors with nZVI to degrade chlorinated compounds [165,166].

As nZVI migrates through the subsurface and approaches the source zone, nZVI surface charge and interfacial tension will impact interactions between nZVI and the contaminant, and hence the reaction rate [154,167]. Enhancing interaction and reaction at the NAPL/water interface requires that nZVI particles exhibit some hydrophobicity, a characteristic not intrinsic to nZVI. Surface coatings can be designed to provide this hydrophobicity, increasing affinity for nZVI to partition to the NAPL–water interface where all reactants are present for contaminant destruction. To reduce the impact of these potential rate-limiting steps recent work has focused on developing nZVI in oil-in-water emulsions such that nZVI degrades NAPL contaminants within the NAPL phase [168,169].

Although some studies have observed a decrease in nZVI reactivity with the addition of a coating [136,139], colloidal stability and mobility of nZVI depend upon polymer coating or other form of stabilizers [157,170]. Thus, injection of nZVI for remediation should consider reactivity as well as the benefits of coatings for mobility in order to optimize the exposure of nZVI to contaminants.

5.5. Impact of natural groundwater constituents and initial chlorinated solvent concentrations

Typical groundwater contains many dissolved electron acceptors (e.g., nitrate or sulfate) that can react with nZVI surface and produce iron surface passivation. The effect of both contaminant and solute concentrations on nZVI performance has been investigated in several studies.

Nitrate (NO_3^-) can strongly influence nZVI reactivity. Liu et al. [138] reported inhibition of TCE reduction by RNIP at high nitrate concentrations ($\geqslant$3 mN) whereas TCE reduction was slightly enhanced at $[NO_3^-] \leqslant 1$ mN. The decreased nZVI reactivity at high NO_3^- concentrations was attributed to competition between NO_3^- and TCE for reactive sites and electrons, and passivation of the nZVI surface due to formation of iron (hydr)oxides. H_2 evolution was also inhibited at high NO_3^- concentrations as Fe^0 preferentially reduced NO^{3-}. Reinsch et al. [133] also reported passivation of RNIP surface at nitrate concentrations of 10^{-4} to 10^{-1} mN, which prevented further oxidation of the Fe^0 for over 6 months.

The effect of other anions such as Cl^-, HCO_3^-, SO_4^{2-} and HPO_4^{2-} on RNIP reactivity was also explored by Liu et al. [138]. Unlike nitrate, these anions had no measureable effect on H_2 evolution. However, they decreased the TCE reduction rate in increasing order of $Cl^- < SO_4^{2-} < HCO_3^- < HPO_4^{2-}$ which is consistent with their affinity to form complexes with iron oxides. This suggests the decreased TCE dehalogenation may be attributed to passivation of the nZVI surface by formation of Fe-anion complexes.

In a study of the effects of anions on dechlorination of 1,2,4-trichlorobenzene by Pd/Fe^{BH}, Lim and Zhu [137] reported a loss in reactivity of Pd/Fe^{BH} with 1,2,4-TCB with the presence of carbonate, nitrate, phosphate, nitrite, sulfite, and sulfide (in increasing order of loss) and with higher concentrations further decreasing reaction rates. Based on the nature of inhibitory effect, the anions were classified as (1) adsorption-precipitation passivating species (phosphate, carbonate), (2) redox-active species (nitrate, nitrite, perchlorate), and catalyst poisons (sulfide, sulfite). The sulfite and sulfide acted as catalyst poisons by diffusing into the bulk of the Pd metal and sorbing onto the Pd sites (also suggested by Lowry and Reinhard [171]).

Heavy metals remediated by nZVI are also influenced by the presence of competitive ions in groundwater. Competitive anions such as sulfates, nitrates and nitrites inhibit metal removal by competing for electrons whereas anions like phosphates and carbonates compete for adsorption sites. Arsenite and arsenate removal by Fe^{BH} decreased significantly in the presence of high concentrations of bicarbonates and phosphates [107,109,111]. Similarly, U^{VI} reduction decreased by 90% in the presence of 1 mM HCO_3^- [113]. Given the complexity of the interaction of groundwater constituents with nZVI, more research is needed to investigate the mechanisms associated with inhibition of removal of heavy metals by nZVI in the presence of various anions.

A number of studies have examined the effect of contaminant concentrations on rates of reaction with nZVI. Higher initial contaminant concentrations increased effective half life values of micro-scale ZVI with time due to surface passivation and saturation of reaction sites [172]. For RNIP, Liu et al. [138] showed that lower reaction rates at later times were observed but only for higher initial TCE concentrations. Liu et al. [12] showed that RNIP particles resulted in lower reaction rates under iron limited conditions (high TCE concentrations) while Fe^{BH} particles shift from pseudo-first order kinetics at low concentrations to zero-order at high TCE concentrations. Liu et al. [12] postulated that either the outer shell on the Fe^{BH} particles remains reactive or that the particles are dissolving leading to exposure of fresh active sites on the Fe^0 surface. In contrast, RNIP particles showed signs of deactivation when TCE concentration increased, likely due to the growth of the Fe_3O_4 shell.

Liu et al. [138] also reported a decrease in RNIP reactive lifetime with higher initial TCE concentrations. The higher TCE concentrations also decreased the total amount of H_2 evolved at the end of the particle's reactive lifetime signifying that RNIP is reducing TCE rather than H^+. Thus, at higher TCE concentrations, most of Fe^0 was used for transforming TCE rather than for forming H_2 by reducing water. This suggests that the application of RNIP particles to NAPL source zones with high TCE concentrations could increase the efficiency of the nanoparticles (as opposed to applying RNIP in low concentration plumes) leading to rapid degradation.

Heavy metals combined with chlorinated solvents are often found as mixed wastes at hazardous sites around the world. The metal co-contaminants undergoing redox reactions may enhance or hinder the removal of chlorinated solvents by nZVI. Some heavy metals (e.g., As, Cr, U) can decrease reactivity by either competing for electrons or precipitating as metal (hydr)oxides on nZVI surface causing passivation. On the other hand, metals like Cu, Ni exhibiting catalytic properties may enhance the nZVI reactivity by forming bimetallic nanoparticles [67,124]. Although extensive research has investigated the effect of metal catalysts on nZVI reactivity, no work has investigated the effect of metal contaminants like As, Cr, or U on nZVI reactivity towards chlorinated solvents.

5.6. Bimetallic nanoparticles

As with monometallic nZVI, bimetallic particles were first used with micro scale iron, e.g. [173–175]. Bimetallic particles are composed of a corrosive metal such as iron or zinc along with a noble metal such as palladium (Pd), platinum (Pt), nickel (Ni), silver (Ag) or copper (Cu). The noble metal is a catalyst and increases the rate of reduction.

Bimetallic nanoparticles can be synthesized in variety of different ways. Wang and Zhang [29] prepared their particles by soaking fresh nZVI particles in an ethanol solution containing a noble metal (Pd, Pt, Ni, Ag, or Cu). Alternatively, the noble metal can be added through a water-based approach [16,157] where a small amount of salt containing the noble metal is used (e.g., K_2PdCl_6 for Pd). Irrespective of the method of synthesis, the iron reduces the noble metal and the metal deposits onto the iron surface:

$$Pd^{2+} + Fe^0 \rightarrow Pd^0 \downarrow + Fe^{2+} \tag{15}$$

The resulting nanoparticle has a thin discontinuous layer of the noble metal on top of the Fe^0 surface [27,66].

Palladium is the most common reductive dehalogenation catalyst used with nZVI for remediation purposes, e.g. [11,16,21,97]. The addition of a noble metal lowers the activation energy of the reaction, allowing more interactions between the compounds to result in reactions, thus increasing the reaction rate. As a result, bimetallic nanoparticles have been used to catalyze dechlorination of compounds which typically have very slow reaction rates with nZVI (e.g. aromatics and polychlorinated biphenyls (PCBs)), e.g. [11,16,29,99,176].

The reaction rates of nZVI particles enhanced with Pd (FePd) and Ni (FeNi) have been reported to be much higher than those of monometallic nZVI. Tee et al. [140] reported the reaction rate (k_{sa}) of FeNi particles to be almost two orders of magnitude higher than monometallic nZVI for degradation of TCE, similar to Schrick et al. [67] who reported degradation rates for FePd nanoparticles over an order of magnitude faster than nZVI and nine times faster than the FeNi particles for the reduction of TCE. Schrick et al. [67] also noticed that Ni was cathodically protected by the iron, but no long term study was performed to examine whether Ni would be oxidized once all the Fe was depleted. Similarly to Schrick et al. [67], Barnes et al. [66] reported no oxidized species of Pd were observed suggesting that the catalyst remains unchanged during the reaction. Lien and Zhang [98] noted that these increased degradation rates (k_{obs}) only occurred when the particles were 1–5 wt% Pd. If the weight was greater than 5%, no increase in reactivity was observed. This is consistent with Barnes et al. [66] who reported 3.2% Ni as the optimum Ni/Fe ratio for maximum dehalogenation of TCE, while Tee et al. [140] reports 20 wt% Ni would obtain the highest degradation rate (k_{sa}). Application of nZVI suspensions with significant fractions of catalysts at field sites is unlikely given the toxicity of the noble catalysts.

End products following reduction of TCE by bimetallic nanoparticles are typically ethane and ethene. Elliott and Zhang [27] reported complete reduction of TCE in 12 h using FePd nanoparticles with ethene and ethane as the major end products, while with non palladized nZVI, ethene was the end product. Lien and Zhang [11] observed complete dechlorination of PCE in 90 min with FePd, with ethane as the major end product, while TCE degradation resulted in both ethane and ethene production.

The reason for the increased rate of reaction of bimetallic nanoparticles has been debated by several authors. Lowry and Reinhard [171] reported that the second metal (in this case AlPd) catalyzes the dehalogenation reaction, resulting in complete conversion of chlorinated ethenes to ethane at the metal surface without any trace of intermediate compounds (i.e. VC). Elliott and Zhang [27] proposed the creation of galvanic cells on the iron surface, where iron is the anode, and the noble metal acts as a cathode. Li and Farrell [81] suggested that the increased ethene and ethane production (as compared to monometallic nZVI) is due to bimetallic nanoparticles reducing the contaminants (in this case TCE) through β-elimination. Lien and Zhang [177] proposed that a transition state species produced in β-elimination is behind dehalogenation of chlorinated ethanes, similar to [54]. Conversely, Schrick et al. [67] proposed that the mechanism for TCE degradation with FeNi nanoparticles involves the transfer of electrons to the Ni which breaks the Cl–C bond and replaces the halogen with a hydrogen atom (in other words, hydrogenolysis). Lien and Zhang [97] suggest that atomic hydrogen is formed on the noble metal surface and acts as the reducing agent for chlorinated compounds. Tee et al. [140] also hypothesized that the addition of a noble metal leads to the enhancement of hydrogenation (of unsaturated compounds to saturated compounds) due to the presence of atomic hydrogen on the noble metal. This may explain the higher concentrations of ethane as the end product in comparison to when non-bimetallic nZVI is used. Given that all the studies with bimetallic nanoparticles to date use Fe^{BH} particles, and these particles can support hydrogenolysis (unlike RNIP particles where β-elimination governs, Section 3), it is likely that enhanced hydrogenation as well as hydrogen production is the main cause for increased reaction rates. However, given the numerous theories put forward with respect to bimetallic nanoparticles, further studies are needed to address these discrepancies.

The disadvantage of using bimetallic nanoparticles is their potentially short lifetimes in the subsurface due to surface passivation [67]. In addition, FePd bimetallic nanoparticles show significant structural changes leading to decreased reactivity (Section 5.2) [99,148]. Zhu and Lim [99] recommend that Pd be introduced to the nZVI at the time of use, rather than preparing the FePd particles a priori and storing them in order to achieve the highest reactivity. Another disadvantage of bimetallic nanoparticles is the added environmental risk associated with injecting another metal into the subsurface, especially when using FeNi nanoparticles [12,67].

6. Stability and mobility of unstabilized nZVI

Laboratory batch studies have shown that nZVI has significant potential for use in remediating chlorinated compound and heavy metal contaminated sites. One significant obstacle limiting wider application of nZVI is the tendency of nZVI particles to rapidly aggregate and settle out of aqueous suspensions. Agglomeration on a timescale of 2–15 min is common for unstabilized nZVI with rapid settling for the following 30 min, resulting in a more than one order of magnitude decrease in suspended nZVI particle concentrations within 1 h [16,22,74]. Classical Derjaguin, Landau, Verwey and Overbeek (DLVO) theory predicts the interaction energy (i.e., sum of van der Waals attractive forces and electrostatic repulsion forces) between two identical colloids (Fig. 2). As the separation distance between two colloids decreases, attractive (negative by convention) van der Waals forces act on a given colloid. These forces are counteracted by repulsive (positive by convention) electrostatic forces which form an energy barrier when they are larger than attractive forces (Fig. 2b). At close separation distances, the attractive forces exceed the electrostatic forces, creating a primary energy minimum well in which particles become irreversibly attached. Phenrat et al. [74] showed that attractive interactions between nZVI particles are dominated by magnetic attractive forces when colloid separation distance decreases (e.g. shown in Fig. 2.a). This study also showed that magnetic attraction between nZVI particles increases proportionally to particle Fe^0 content and

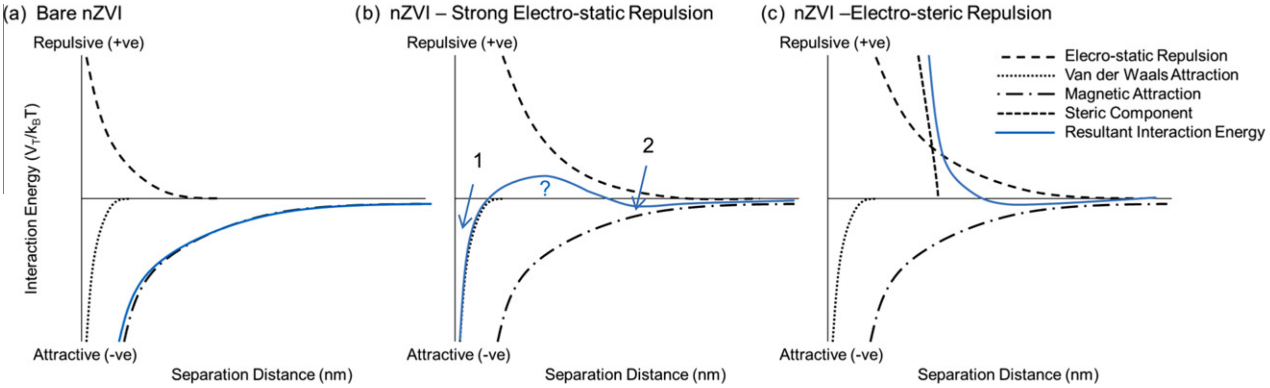

Fig. 2. Conceptual model of DLVO interaction forces for nZVI particles with different surface properties: (a) bare nZVI, (b) nZVI with strong electro-static repulsion and (c) nZVI with both electro-static and steric repulsion. Points 1 and 2 refer to the primary and secondary minimum, respectively.

particle radius to the 6th power [74]. These studies provide insight into particle aggregation but not mobility. Hong et al. [178] examined various iron oxide particles and demonstrated that nanoparticles with high magnetic moments exhibit poor mobility in porous media due to rapid particle aggregation. Limiting particle aggregation and settling is a prerequisite for enhanced migration.

Many nZVI studies were conducted at relatively low nZVI concentrations (lower than would be expected during field applications) [179]. Increasing nZVI concentration (volume fraction) results in closer range interaction forces between particles, increasing aggregation [74]. It has been suggested that above 0.015 g/L aggregation is expected to play a role in nZVI stability [180], which is consistent with stability observations [74]. A recent study suggests large aggregates play a strong inhibitory role in nZVI colloidal stability due to the very long range of magnetic forces in solution [180].

Poor stability and mobility has been observed in column experiments that evaluate unstabilized nZVI transport [158,167] due to the absence of a sufficient electro-static energy barrier to prevent large aggregates from forming and depositing [181]. These experiments were performed at relatively low concentration (0.1–0.3 g/L) nZVI. Delivering nZVI through porous media becomes more challenging when higher concentrations are used and aggregation becomes more rapid. Field applications of nZVI typically have used over an order of magnitude higher concentration (1.0–30.0 g/L) [18,25,26,182–184] and have encountered problems with limited nZVI mobility likely due to extensive nanoparticle aggregation and retention.

6.1. Improved colloidal stability

Recognizing the strong interaction between nZVI particles, researchers have devoted considerable effort to the development of surface modifications to minimize aggregation and settling, thereby increasing nZVI mobility in porous media. To this end, desirable characteristics of nZVI slurries include: (1) particles that do not rapidly aggregate, thus are a stable size and do not settle; (2) particles that contain enough zero valent content and surface area for reaction upon delivery; (3) stabilizer characteristics that do not negatively affect injection or reactivity while providing stability and mobility in porous media.

There are two widely adopted methods for stabilization of nZVI particles: nZVI stabilization following synthesis, or inclusion of a stabilizer in the suspension during nZVI synthesis, as discussed in Section 3.4. There is a large body of literature focused on characterizing and stabilizing nZVI particles that have been previously synthesized and allowed to aggregate [22,110,158,159,185,186]. This technique uses ultra-sonic probes and baths to apply a sufficiently high energy to dis-aggregate nZVI particles. Stabilizing agents are then physically adsorbed to the surface via mixing. Many polymers have been successfully used to stabilize nZVI using this technique, the most successful of which are high molecular weight anionic polyelectrolytes (e.g., poly-styrene sulfonate, polyvinyl pirolidone) [187]. Naturally occurring organic matter may serve the same stabilizing function [186]. The polymer provides a "brush" that both provides electro-static repulsion due to the charge on the polymer and physically inhibits permanent aggregation upon intra-particle interaction due to steric repulsion [20]. Fig. 2c shows the DLVO and magnetic force considerations for nZVI as well as the physical mechanisms of intra-particle repulsion afforded by polymer coating, including electro-static and steric repulsion. The main advantage of the post-synthesis stabilization methodology is that unstabilized nZVI is a more economical choice. nZVI that is re-suspended has a passivated oxide shell which protects the zero valent iron core from further oxidation, allowing reasonable shipping and holding times [188]. The disadvantages are that, in addition to the laborious and lengthy process of stabilizing particles, a large fraction (by weight) of the nZVI particles cannot be effectively stabilized [76]. Dense surface polymers necessary to stabilize re-suspended nZVI inhibit reaction with contaminants [136].

Similar post-synthesis stabilization methods have been tested for other polymers. Guar gum was investigated as an alternative polymer [159,181] providing similar stability to previously studied anionic polymers. Commonly used as an additive in drilling and hydraulic fracturing, guar gum molecules do not have charged functional groups to contribute to electro-static repulsion, but provide steric repulsion. This shows that the electro-static interaction is less important for screening magnetic attraction forces for post-synthesis stabilized nZVI than steric repulsion. Shear thinning polymers like Xanthan Gum (Xg), previously used for the delivery of microscale ZVI for remedial purposes [189], have also been suggested as a suitable stabilizer [190]. This approach produces very stable nZVI particles (on the order of weeks without agglomeration and settling) due to the creation of gelling (or networking) between individual particles that inhibit interaction [191]. This approach is advantageous when very high concentrations of nZVI need to be injected (>15 g/L nZVI). However, due to the high polymer content (0.3–0.6 wt% Xg) the injection solution can be very viscous (approaching 1000 cP at shear rates below 1 s^{-1}) complicating injection conditions due to large pressure required for injection. Adsorption of hydrophilic carbon, another variation of post-synthesis stabilization, has also been reported [158,192] and shown to improve stability and mobility of nZVI compared to bare nZVI.

The second method for nZVI stabilization involves a modified chemical precipitation process in which the presence of the polymer stabilizes nZVI particles as they are precipitated from solution (presynthesis). This method, developed by researchers at Auburn University [16], has been most widely used with CMC. This polymer controls nZVI nucleation limiting aggregation during synthesis [21,138,157]. The presynthesis stabilization process has been shown to yield very stable nZVI solutions for select anionic polymers [21] that can provide electro-steric repulsive interactions. In addition, the process facilitates manipulation of particle size [17]. Enhanced ultra-sonic mixing techniques during synthesis in the presence of a high molecular weight polyvinyl acid can be used to control particle size, breaking up large particles [23]. This additional step produced very small nZVI particles that were reportedly stable in solution for months. Composite nanoparticles containing zero valent iron (i.e. nZVI in a silica matrix) have also been synthesized as a delivery vehicle [24,156]. nZVI particles, grown on stabilizing media have also been presented [161] to improve PRBs. An extension of this is the incorporation of nZVI particles into reactive membranes [163] with potential applications in industrial water and wastewater treatment.

The use of nZVI emulsions have also been presented as a method of limiting particle–particle and particle–soil interactions [26,179]. Using this modified post-synthesis approach, nano or micro scale iron particles can be stabilized through their encapsulation in biodegradable oil with the aid of a surfactant. The EZVI process effectively encapsulates nZVI slurry in an oil phase utilizing viscosity and surface tension to prevent particle settling [26]. One concern with this approach is that nZVI emulsions have a very high viscosity (>1000 cP) and would necessitate elevated injection pressures. Recognizing this problem, in a more recent study the highly viscous vegetable oil in the emulsion was replaced with oleic acid, producing less viscous nZVI emulsion slurries [179]. This oil in water emulsion method separates nZVI and water in the emulsion, preventing oxidation. An important consideration with using emulsions to transport nZVI is the integrity of the emulsion droplets under high shear conditions present at the well screen, which could potentially destroy the effective mechanism of nZVI stability. In addition consideration of the droplet sizes is important to avoid pore straining which would negatively impact mobility (i.e., emulsion droplets must remain smaller than the pores to be mobile) [179].

6.2. Bench scale experiments investigating nZVI mobility

In order to make nZVI economically feasible a considerable amount of the injected nZVI mass must reach the contaminated source zone. Small scale column tests are commonly used to evaluate nZVI mobility under a range of representative subsurface conditions. Such experiments have been used to study the transport of numerous environmental colloids, e.g. [193–195], as well as other engineered nanoparticles [196], nC_{60} particles, [197] and carbon nanotubes [198].

Several column experiments have been conducted with unstabilized nZVI; however mobility was limited [158,181,186]. Subsequent studies showed that mobility can be improved when the nZVI surface is modified to provide electro-steric repulsion [20,110,156,185–188,192]. Phenrat et al. [20] measured the steric layer properties of several polymers adsorbed to nZVI and demonstrated that the same steric repulsion that limits aggregation also increases nZVI transport through porous media by limiting particle-soil interactions. Very high mobility has also been reported in column experiments performed with nZVI prepared using a presynthesis stabilization technique with CMC polymer that provides electro-steric repulsion [170]. It has also been demonstrated in transport experiments that both methods of providing electro-steric stabilization (pre and post synthesis) still provide good stabilization even in solutions of high ionic strength and divalent cations [170,187]. Studies also show that naturally occurring organic matter subsurface constituents may act in a similar fashion to surface modifications, potentially increasing the mobility of nZVI [186] as with other colloids [199].

Although significant advances have been made in improving nZVI mobility in porous media, many early transport studies were conducted using conditions that did not adequately represent subsurface conditions. Experiments were typically conducted at unrealistically high pore velocities. Another limitation of these early studies is the low nZVI concentrations (less than 0.25 g/L) that were used. According to the USEPA voluntary database of past and future nZVI field injections; concentrations on the order of 1–30 g/L are utilized in the field [25,200]. Results from column experiments conducted at low nZVI concentrations may not be directly applicable to field application scenarios using much higher nZVI concentrations. More recent column experiments have been conducted at higher concentration injections, providing more relevant information for nZVI application. Phenrat et al. [76] demonstrated that higher concentrations of post-synthesis stabilized nZVI could be transported through porous media, although transport was limited by aggregation of nZVI more than nZVI interaction with the porous media. At high nZVI concentrations nZVI particles collide more frequently and are attracted to one another, depositing in the secondary energy minimum, forming larger aggregates. Particles trapped in a secondary minimum (Point 2 in Fig. 2b) are weakly attached as opposed to those in primary minimum that are irreversibly removed from solution (Point 1 in Fig. 2a). nZVI particles deposited in the secondary minimum can detach/disaggregate due to fluid shear or diffusion [76]. Low concentration nZVI suspensions have higher particle diffusion resulting in disaggregation rates that can approach aggregation rates. To limit nZVI deposition in the secondary minimum and hence limit aggregation, polymers should be chosen to maximize long range electro-steric screening resulting in only a shallow secondary minimum (e.g. Fig. 2c).

Another important design consideration for optimal mobility is particle size. Elliot and Zhang [27] suggested particle diameters of between 100 and 200 nm [27] to optimize mobility at typical groundwater velocities and limit nZVI retention in porous media due to physicochemical filtration [195,201]. Mobility is limited by deposition due to diffusion when particles are smaller than this range and gravity deposition becomes limiting for mobility when particles are larger than this range. In addition, the particle size in this case is not necessarily the individual initial nZVI particle size if particles are growing to form stable aggregates [178]. However, many other factors affect this optimal range including injection velocity, porous media grain size, and solution viscosity, and should thus be included in design considerations along with particle size.

One of the main limitations of many column studies to date is the range of velocities used. Typical groundwater velocities range on the order of 0.1 m/day under natural conditions to 10 m/day in a typical remediation scenario with an imposed hydraulic gradient [27,179]. Subsurface heterogeneity results in significant variation in hydraulic conductivity (K), resulting in low permeability zones where groundwater velocity will be even lower than 0.1 m/day, limiting nZVI mobility. Column experiment pore velocities ranging from 15 to 35 m/day [76,170,185] up to 260 m/day have been reported [156,191,202]. Although these experiments are quicker to complete, they are not representative of nZVI transport at field sites. There have been several recent column studies reporting high concentration nZVI injection at realistic pore velocities. Berge and Ramsburg [179] reported column experiments showing good mobility of nZVI emulsions at velocities of 0.4 m/day, a velocity that could occur within a few meters of an injection well [179]. Their nZVI suspension viscosity was 2.4–9.3 cP which would be within an acceptable range for field injection. Mobility has varied at low pore velocities in other studies. Post-synthesis stabilized nZVI (using guar gum) had limited mobility as velocities decreased to 2 m/day [181] whereas, presynthesis stabilized nZVI (using CMC polymer) was reported to be mobile at low velocities (0.1–2 m/day), and at higher concentrations (3 g/L) [203].

Previous studies that utilized high pore water velocities for nanometal delivery typically did not consider the prohibitively large injection pressures required to achieve these velocities. Vecchia et al. [191] studied the transport of shear thinning polymers for nZVI delivery and recorded pressures exceeding 60 kPa in column (46 cm long) experiments using highly viscous injections. Berge and Ramsburg [179] discussed the effects of viscosity on injection and the need to minimize solution viscosity, optimize velocity and minimize pressure during field scale injection, discussed in Section 8.2. Recent work has also suggested that the high shear in column experiments, believed to encourage disaggregation (or re-suspend nZVI deposited in a shallow secondary energy minimum), may not occur when multidimensional experiments are conducted due to the additional flow paths provided [19]. Although column studies are unable to replicate all of the complex phenomena occurring at the field scale they are an important step in building and validating conceptual models for the prediction of nZVI transport. Ultimately, these experiments will aid in the design nZVI injection at field sites, especially when they are performed under representative subsurface conditions.

6.3. NAPL targeting

Limiting interactions between nZVI and porous media is desirable to maximize nZVI mobility. However, once nZVI has reached the target contaminated zone, sufficient residence time is required to allow completion of reactions with contaminants. This can occur due to deposition of nZVI on soil in the contaminated zone, or due to partitioning of nZVI to the NAPL–water interface. As nZVI is typically stabilized in an aqueous phase it has a limited affinity for NAPL. Several studies have investigated the ability of surface modifiers to “target” NAPL, or preferentially interact with non-polar species. EZVI was designed to surround ZVI by an oil–liquid membrane that will absorb free phase NAPL bringing nZVI and NAPL into proximity [26]. Reductive dechlorination associated with nZVI requires that water (or another proton donor) be present. Thus, nZVI will be the most reactive at the interface of NAPL and water. Partitioning of nZVI the NAPL–water interface has been achieved using hydrophilic and hydrophobic polymers adsorbed to the nZVI, reducing the energy of this surface. These formulations had an increased affinity for hydrophobic coated sand grains [167]. A study evaluating the targeting tendencies of more widely used and inexpensive polymers (e.g., PAA, CMC) [154] suggested that ideal polymers would maintain low interaction with soils to enhance transport and exhibit slight hydrophobicity to increase affinity for NAPL. Berge and Ramsburg [179] developed an nZVI emulsion that was hydrophobic, and could partition to NAPL. They were able to achieve reductive dechlorination within a NAPL using an nZVI emulsion. Consideration of the potentially negative impacts of DNAPL mobilization and subsequent sinking, especially when using high injection pressures, surfactants, and high viscosity solutions, need to be considered when using any of these NAPL targeting techniques [179].

7. Simulation of nZVI transport

Numerical models can be valuable tools for design of remediation schemes at contaminated sites. Once validated, these models can reduce the need for costly treatability studies and avoid costly errors such as the implementation of inappropriate or ineffective remediation methods. To date, no comprehensive numerical model has been developed for the prediction of nanoparticle transport and remediation. The limited model development to simulate nanoparticle transport and reactivity completed to date has been predominantly applied to small batch experiments or one-dimensional column experiments [12,66,156,158].

Many of the models developed are based on colloid filtration theory (CFT), which was originally developed for water treatment [204] and has been widely used to describe physicochemical filtration in porous media. The colloid filtration process is incorporated into the advection-dispersion equation as a first order attachment term:

$$\frac{\partial C}{\partial t} = D_H \frac{\partial^2 C}{\partial x^2} - v_p \frac{\partial C}{\partial x} - K_{Att} C \tag{16}$$

where C is the nZVI concentration in the solution (M/L^3), D_H is the hydrodynamic dispersion (L^2/T), v_p is the pore water velocity (L/T), t is time (T), K_{Att} is the rate at which nZVI attaches or is deposited on available collector sites (1/T).

$$K_{Att} = \frac{3(1-\theta_w)}{2d_{50}} \alpha \eta_o v_p \tag{17}$$

where d_{50} is the median collector grain size (L), θ_w is the volumetric water content (–) and η_o is the theoretical collision efficiency (–). η_o is defined as the ratio of particles striking a collector to those approaching the collector. It is calculated by considering the cumulative effects of diffusion (i.e., Brownian motion), interception, and gravity on the particle as it passes by an ideal collector, e.g. [195,201,204]. The dimensionless parameter α is the sticking efficiency (–), which is the ratio of colloids that stick to the collector to those that strike the collector. η_o can be estimated using a variety of approaches [195,201,204,205] whereas α is typically a fitting parameter. Many researchers use the steady state analytical solution to Eq. (17) to quantify the sticking efficiency in nanoparticle mobility studies:

$$\alpha = -\frac{2}{3} \frac{d_{50}}{(1-\theta) L \eta_o} \ln(C/C_0) \tag{18}$$

where L is the length of porous media (L), and C/C_0 is the maximum normalized effluent concentration.

A number of studies have used CFT to interpret results from column studies and extrapolate to maximum nZVI travel distance in the field (calculated as the distance needed for nZVI concentration to reduce to 0.1% of the initial concentration). Column studies have used bare nZVI [158,181,186], postsynthesis stabilized nZVI [76,158,167,181,186,191] as well as presynthesis stabilized nZVI [170,203]. One common method to compare experimental results has been to compare the sticking coefficient fitted using Eq. (18). Fitted sticking coefficients have ranged from 0.1 to 1.0 for bare nZVI, 0.002 to 0.07 for postsynthesis stabilized nZVI and 0.0003 to 0.0023 for presynthesis stabilized nZVI [76,158,170,186]. Application of Eq. (17) assumes that nZVI particles are stable in suspension (i.e., no aggregation or settling). A number of studies have found that this is not the case. At high nZVI concentrations (above 1 g/L), aggregation and deposition can become a dominant removal mechanism in comparison to particle–soil interactions, due to the increased number of particle/particle interactions [76]. Given that CFT does not account for particle–particle interactions, it should be used with caution for the prediction or interpretation of unstable nZVI transport [76]. It should be noted, however, that studies have been able to interpret some nZVI transport experiments using CFT since nZVI was colloidally stable in these studies [170].

A goal of several studies has been to improve the understanding of particle aggregation or temporal changes in aggregate size, with an ultimate goal of modifying Eq. (17) to incorporate particle aggregation. A recent study shows that consideration of nZVI size change with time improves interpretation of nZVI transport in column experiments [203]. Hong et al. [178] observed that stable aggregates formed in proportion to the total magnetic interaction and proposed that use of the stable aggregate size, as opposed to the individual nZVI particle size, would be more appropriate for the estimation of the collector efficiency (η_o). A study of iron oxide nanoparticles indicated that the size of particles during aggregation and disaggregation can be mathematically described using an exponential decay function [206]. This work supports earlier experimental work by Phenrat et al. [74] who showed that unstabilized nZVI quickly aggregated and settled in time resolved UV-light absorption experiments. Models based on the solution of Eq. (17) can utilize this relationship, updating η_o to reflect the aggregating particle size in time. It has also been shown that the aggregation rate increased with larger initial particle size [180].

Phenrat et al. [207] developed an empirical correlation for changes in nZVI aggregate size during transport in porous media. However, this correlation requires specification of a large number of system parameters (e.g., geologic, hydrologic, and geochemical) in addition to a number of small scale parameters that can vary widely depending on subsurface conditions. Given that this correlation was calibrated for a reasonably small range of the parameters, model prediction would likely only be valid within the calibration range. Another study has proposed a statistical approach to account for bimodal particle size distributions requiring solution of the CFT equation for each particle size subpopulation [208]. More research is needed to develop more fundamental understanding of the nZVI aggregation processes.

Not all studies have applied CFT to predict nZVI transport. Kanel et al. [209] successfully used SEAWAT [210] to predict the downward migration of nZVI, due to density contrasts, observed in 2-D sandbox experiments. However, SEAWAT simulates density effects associated with dissolved salts, not suspensions of particles. Other variations of the nZVI technology that will require a novel modeling approach include the simulation of viscosity changes associated with shear thinning fluids in the stabilization suspension [202]. Prediction of nZVI transport, whether or not in the framework of CFT, must also account for particle-particle as well as particle–collector interactions.

Although many studies have simulated nZVI transport in controlled laboratory experiments, there are currently no published modeling studies of nZVI transport at the field scale. Before nZVI fate and transport models can be confidently used in design of field scale remediation, the models need to be validated using data from well monitored field investigations. Given the complex redox reactions involved in nZVI remediation, it is likely that there will be a need for the development of models that will go well beyond simple application of CFT and include particle-particle interactions, particle–soil interactions, and reactions with contaminants and other groundwater constituents.

8. nZVI field applications

The first field scale injections of nZVI used unstabilized nZVI leading to limited mobility [27]. More recent field scale studies have utilized a variety of stabilizers, improving nZVI transport [18,25,184,211]. Although nZVI has been injected at a number of sites, many of the test sites reported in a recent EPA database (26 in total) do not have associated publications or technical reports [212]. Details from 8 studies have been presented in academic journals and limited information has been provided for 13 others in the form of conference papers, conference presentations, reports, and other technical reports that have been made publically available but not peer-reviewed. According to a recent report published by the National Institute of Environmental Health Sciences there have been 44 sites worldwide where nano-materials have been injected into the subsurface for remediation purposes [213]. With the growing number of bench scale feasibility studies reporting mobile nZVI, this number is likely to grow.

8.1. Early studies of nZVI in the field

Initial nZVI field studies used unstabilized nZVI [27,28] that has since been shown to rapidly aggregate and settle out of suspension [74]. In the field, this translates into rapid deposition of nZVI within the wellbore, limiting mobility. In one field study nZVI was injected at 1.5 g/L; however, only 10–20 mg/L (expressed as total Fe) reached monitoring wells at a distance of 1.5 m [27]. Poor mobility on the order of a few inches to a few feet was believed to be due to clogging of the well screen by nZVI aggregates [23]. Discrete nZVI particles, present as zero valent iron, were not distinguished from soluble iron corrosion products. It is likely that much of the downstream iron quantified was soluble iron corrosion products that dissolved near the injection well screen and flowed to the monitoring location. In a subsequent study nZVI was injected into a highly conductive fractured bedrock with a reported estimated radius of influence from the injection to be 6–11 m based on ORP readings, although the ORP readings outside the injection well rebounded shortly after injection [28,214]. Recent work has questioned the interpretation of ORP data as evidence of successful nZVI emplacement during field application, suggesting that the highly complex redox response indicates nZVI corrosion and transport of these corrosion products and not transport of the nZVI particles themselves [215]. Early studies evaluating nZVI injection only briefly address mobility and delivery, primarily focusing on reaction of target contaminants. Target VOC removal efficiencies were reported to be 36–96% [28,214], where removal efficiency is defined to be the observed aqueous phase VOC concentrations normalized to the baseline concentration. These removal efficiencies were sustained for three months, although the most successful results were observed in the injection well.

To effectively monitor remediation, more rigorous monitoring will be required as concentrations within the injection well are not an accurate indication of formation contaminant concentrations. In many studies nZVI likely deposited in the well screen, and monitoring VOC degradation at the injection well may only have been measuring degradation through the well screen, which effectively acted as a PRB. In one study [214], VOC concentrations in the monitoring well 6 m down gradient continued to decrease for two months after injection, although the contributions of up gradient reaction with nZVI and biological activity, followed by transport of degradation products downstream, is not discussed. The evaluation of the success of nZVI delivery in field scale applications is further complicated by widely spaced monitoring well locations and the inability to directly identify nanoparticles, relying instead on indirect evidence of nanoparticle transport (e.g., ORP).

These first studies were reported as successes with limited discussion addressing challenges associated with nZVI application at the field scale [27,28,214]. There is a significant need for field studies that demonstrate rigorous site characterization, optimization of on-site injection infrastructure, design of injection fluid properties, and reporting methods in order to reduce the uncertainty associated with nZVI delivery.

8.2. Improvements to field scale nZVI delivery

Rapid nZVI aggregation in early field studies likely caused nZVI to travel less than a meter upon injection [23], partially contributing to nZVI not being widely accepted in the remediation community. Several field scale studies have been conducted to evaluate the use of stabilized nZVI, with promising results in comparison to early studies [18,25,184,211]. These studies have used nZVI injection concentrations ranging from 0.2 to 30 g/L [18,25,26,182–184]. However, field studies to date lack definitive evidence of nZVI mobility at the intended radius of influence and uniform nZVI spreading within the treatment zone.

Henn et al. [211] observed "black stained" water, a color indicative of nZVI, in a monitoring well 1.06 m from an injection point. Post-injection slug tests confirmed that the injection wells were not significantly impacted by well clogging, suggesting the nZVI was mobile. However, at other monitoring points, located between 0.75 and 1.5 m from injection wells, no black color was observed. Other studies report lower than expected travel distances using postsynthesis stabilized nZVI, e.g. [182,216] and nonuniform travel to target monitoring wells, e.g. [200]. A recent study reported that stabilized nZVI was mobile in a field test traveling 3 m to a monitoring well, aided by a very high 20 L/min injection rate [184]. However, nZVI was not well distributed throughout the targeted depth of contamination. Most of the nZVI appears to have travelled through a preferential pathway comprised of coarse sand due to a 15 m screened interval in the injection well.

In the case of He et al. [18], high mobility of presynthesis stabilized nZVI was demonstrated during a field study using two injection conditions. Using gravity feed and pressurized injections nZVI was observed in a monitoring well 1.5 m down gradient at breakthrough concentrations of 37% and 70% respectively (when normalized to the tracer) [18]. Use of tracers is important for the validation of nanoparticle transport models and in the determination of nZVI deposition in the subsurface. Their study also reported that nZVI was not detected in a monitoring well 3 m down gradient. However, this well was screened at a depth 1.5 m above the injection well, suggesting that the nZVI may have moved vertically as it travelled horizontally. In summary, stabilized nZVI has been visually confirmed to travel 1 m from an injection well, although evidence suggests that maximum travel distances of up to 2–3 m may be achieved in high permeability formations.

Careful control of the hydraulic conditions, and therefore groundwater velocity, is essential for delivery of nZVI. There is evidence to suggest that under ambient groundwater conditions even the most stable nZVI is effectively immobile. Bennett et al. [25], performing a push-pull field test, observed a significant loss of mobility after a 13 h lag period (i.e., no applied gradient resulting in a pore water velocity <0.3 m/d) [25]. This nZVI formulation has been shown to be highly mobile in column experiments [170] and exhibited good mobility in two other push pull tests in this field study [25], suggesting that groundwater recirculation and other methods to promote nZVI spreading in previous studies [182,211] may be a necessity for nZVI delivery.

The addition of stabilizers to nZVI suspensions can result in colloidally stable nZVI that can be transmitted through porous media; however the addition of stabilizer also affects fluid properties (e.g. viscosity, interfacial tension) of the injection fluid. Solution viscosity has been reported in very few studies, but can range from slightly above water (e.g. 5–20 cP) to much higher viscosities (e.g. 1942 cP [26]), having a significant impact on injection. Increased solution viscosity resulting from stabilizers can increase the head in the injection well, at constant injection rates, or reduce injection velocities given a constant injection head. Reported injection pressures during field studies have ranged from low to moderate (e.g. <34.5 kPa [18] to 137.9 kPa [200]) in some injections, but have reached higher pressures (e.g. 344.7 kPa [183]) when the viscosity of the nZVI suspension is greater.

Highly viscous suspensions can be advantageous to mitigate against viscous fingering during pressurized injection and have been demonstrated to emplace EZVI with a reported radius of influence of 2.13 m [183] compared to 0.45 m using gravity feed. However, it has also been suggested that highly viscous nZVI suspensions are capable of mobilizing NAPL even at moderate injection velocities [179], which should be considered in the hydraulic design of the injection. Another consideration in manipulating the flow field is the depth of injection and potential daylighting [183], which renders the injection well unusable for subsequent injection. Recent nZVI injections have been successful in comparison to early field injections which had limited nZVI mobility due to aggregation. However, unpredictable mobility and inconsistent subsurface distribution continue to pose problems upon injection.

8.3. Tracking remediation following nZVI injection

Many nZVI field trials have been reported as successes but direct comparison of these studies is challenging, as data reporting is inconsistent. As was the case with comparison of bench scale column experiments, comparing pilot scale studies is complicated due to the use of different types of nZVI, different stabilizers, different injection conditions (e.g., injection pressure and rate, injection well screen length) as well as injection into different geologies (e.g., fractured rock, sandy aquifer material, and low permeability media). It is important to develop metrics of nZVI injection success as well as remediation to facilitate a comparison between field studies and provide an impartial assessment of this remediation technology.

There are many uncertainties associated with field scale application of nZVI. One significant need is for methods to directly identify and quantify nZVI (among other nanoparticles [217]) in environmental systems. Knowledge of the extent of nZVI migration is required to determine if the injected nZVI is reaching the target treatment zone. Currently, nZVI transport is often tracked by observing changes in aqueous geochemistry caused by nZVI reactions [18,27,184]. ORP, pH, total iron, suspended solids, total solids, and dissolved oxygen (DO) have all been suggested as indicators of nZVI at field sites. However, none of these parameters alone directly confirm the presence of nZVI particles. The problem with these indirect indicators of nZVI presence is that they do not distinguish between nZVI particles and dissolved corrosion species and associated geochemical changes. Due to the significant iron corrosion and dissolution this becomes important at the field scale. Separation of dissolved iron species and nZVI particles is problematic as stable nZVI particles (e.g. 20 nm) have been reported to pass filters (e.g. 0.45 μm) commonly used to distinguish dissolved and total iron [25]. This suggests that methods must be improved to distinguish dissolved iron species from stable nZVI particles in field samples.

Changes in ORP have been commonly used to indicate the presence of nZVI in field studies [27,28,150,184,214] as it becomes strongly negative following application of nZVI due to iron oxidation (e.g. decreasing to −360 mV and −700 mV in the injection well following nZVI injection). However, one study [182] observed no change in ORP after injection, likely because a highly concentrated nZVI solution was diluted with tap water that had a high dissolved oxygen content so that the surface of the iron would have been oxidized prior to injection and no further iron oxidation occurred *in situ*. In some cases ORP response has been interpreted as successful delivery of nZVI [18,184]. However, a recent study investigating the temporal evolution of ORP impact from nZVI has reported that even low concentrations of nZVI (e.g. <50 mg/L) can lead to significant reductions in measured ORP [215]. The study reports that at low nZVI concentrations ORP readings are a mixture of contributions from nZVI as well as dissolved reaction products (e.g. H_2 and Fe^{2+}) [215] which will have different transport characteristics. They also found that with increasing nZVI concentration, ORP readings were influenced by the adsorption of nZVI to the ORP probe [215]. This implies that presence of nZVI in environmental samples should not be based solely on ORP but on multiple lines of evidence.

Other geochemical parameters that have been associated with the presence of nZVI in field samples include pH and DO. Oxidation of nZVI in aqueous solution increases aqueous phase pH (Eqs. (6) and (7)) and can lead to the consumption of oxidants (e.g. dissolved oxygen). Several field studies have noted pH increases following nZVI injection [27,28,214], and in some cases has been suggested as an indicator of the nZVI migration front [184,211]. However, two nZVI field injections resulted in no significant pH change after injection [182,211]. It is difficult to draw conclusions from these conflicting reports, as groundwater chemistry can vary widely (e.g. buffering capacity, oxidant species), and there are other compounding reactions in the subsurface that can influence pH. Decreases in DO have been observed following nZVI injection in several field studies [18,27,182,211]. However, similar to the discussion related to ORP, low DO measurements may be the result of upstream nZVI corrosion and subsequent downstream migration. As such they may not indicate the presence of nZVI.

Success in remediation studies is often based on decrease in total aqueous VOC concentrations, with reported decreases greater than 90% in injection wells [218], in some cases persisting for months after injection. Other studies have reported similarly high target contaminant removal efficiencies (e.g. 50–99% removal of vinyl chloride [184]) and have gone so far as to declare site closure or recourse to monitored natural attenuation following nZVI injection, e.g. [200]. However, aqueous phase contaminants can be displaced by the injection fluid, pushing contamination out of the treatment area [25,211]. These studies imply that earlier studies that report aqueous VOC removal within monitoring and injection wells need to account for the transfer or displacement of contaminated groundwater out of the study area after injection. This displaced water with high VOC concentrations can flow back to the treatment zone under ambient flow conditions, resulting in rebounding VOC levels as observed by Mace [218]. For this reason it has been suggested that nZVI is best utilized when the majority of contamination exists in a stationary phase (NAPL or sorbed phase contamination, not aqueous phase [25]).

Another uncertainty in evaluating remediation of chlorinated solvents using nZVI is determining the contributions from abiotic and biotic degradation. nZVI injection creates reducing conditions in the subsurface that are favorable for bioremediation [18,27,184,211,218]. Injection suspensions commonly contain a polymer (or other substrate) that is readily biodegradable. Rapid decreases in VOC concentrations are typically associated with abiotic degradation [18,26,211]. However with time concentrations may rebound over an intermediate period [18,211,218] prior to the onset of biodegradation [18]. Other studies report similar long term declining VOC trends and increases of reaction products, confirming that some remediation occurs up to 19 months after nZVI injection [26]. There is a need to better distinguish abiotic and biotic degradation and to determine the impact of nZVI on biological activity to assess the utility of applying nZVI over some other type of biostimulation technology.

There are many groundwater constituents that interact with nZVI; however many of these interactions are not well understood or otherwise cannot be individually isolated in natural systems. The presence of naturally occurring groundwater species (e.g. nitrate, nitrite, sulfate) are examples that may affect nZVI reaction. Interpretation of data in the field is further complicated by reaction products from bioremediation [18,26,211] as well as processes that dilute and disperse groundwater constituents. Due to the complexity of subsurface biogeochemistry, analysis of dissolved light hydrocarbons (e.g. methane), anions (e.g. nitrate, sulfate), volatile fatty acids, as well as total organic carbon, have become common baseline analytes to evaluate bioremediation in field studies utilizing nZVI [183]. This is in addition to analysis of VOCs, anions, ORP, pH, total iron, suspended solids, total solids, and DO. No supporting studies to date have presented evidence to suggest that application of nZVI will elicit a predictable and reliable response from any of these parameters, given pre-injection biogeochemistry.

To draw conclusions about remediation, an extensive monitoring plan is often used employing many of the aforementioned parameters. Field studies have sampled daily to weekly to evaluate abiotic remediation [18,25,184,211], and quarterly to biannually to evaluate nZVI induced bioremediation [18,26,183,184,211]. Though with relatively few supporting lab studies that investigate the complex effects of nZVI with constituents in the subsurface, e.g. [215], it is difficult to conclusively evaluate nZVI performance. Future nZVI pilot projects should complement field monitoring with supporting bench scale experiments and investigations to fill the knowledge gaps in nZVI implementation including the effect of nZVI on pH, DO, ORP, dissolved Fe, and other groundwater constituents. There is also a need for field investigations to demonstrate the technology using established field techniques in order to develop definitive metrics of success for field scale injection. These studies would aid in informing practitioners of effective methods to monitor and apply nZVI in the field, leading to successful remediation.

9. Summary and outlook

Significant potential has been demonstrated for the application of nanometals for the remediation of a wide range of priority pollutants in controlled laboratory experiments. However, nanometal technology has not achieved widespread commercial application for a number of reasons. Rapid aggregation and settling of nZVI, leading to poor subsurface mobility has been a problem. In addition, reaction of nZVI with a number of natural groundwater constituents has led to decreases of the reducing equivalents available for reaction with the target contaminants. These problems pose the greatest challenge to the nZVI technology, resulting in ineffective delivery of nZVI particles to the contaminants and reducing the effectiveness of nZVI. Another issue is the high cost associated with synthesis of nanometals for field application. This cost continues to decrease as new sources of nanometal raw materials are found (e.g., new suppliers, alternative raw materials). Lastly, displacement of dilute contaminant plumes upon nZVI injection has been observed at some sites, suggesting that nZVI technology may be better suited to source zones rather than dilute plumes.

Additional research is needed at all scales (i.e., nanoscale to field scale) to improve the understanding of the potential of nanometals for remediation. At the nanoscale, an improved understanding of the governing chemical reactions and physical mechanisms governing transport will ultimately translate into success at the field scale. More field applications are required with detailed characterization before and after nZVI injection to assess nZVI mobility and the extent of contaminant destruction. All of this information will aid in the development and validation of numerical models that can be used to predict remediation at a wide range of field sites.

The research and development to date highlights the significant promise of nanometal technology for contaminated site remediation. Future research in nanotechnology is expected to lead to new advances in bimetallic particles, improved stabilizers, and improved formulations for enhancing partitioning of nZVI to NAPL.

References

[1] Fruchter JS, Cole CR, Williams MD, Vermeul VR, Amonette JE, Szecsody JE, et al. Creation of a subsurface permeable treatment zone for aqueous

chromate contamination using in situ redox manipulation. Ground Water Monit Remed 2000;20:66–77.

[2] Ramsburg CA, Pennell KD. Density-modified displacement for DNAPL source zone remediation: Density conversion and recovery in heterogeneous aquifer cells. Environ Sci Technol 2002;36:3176–87.

[3] She HY, Sleep BE. Removal of perchloroethylene from a layered soil system by steam flushing. Ground Water Monit Remed 1999;19:70–7.

[4] USEPA. Solidification/stabilization use at superfund sites. Cinnacinati, OH: United States Environmental Protection Agency; 2000. EPA-542-R-00-010. <http://www.epa.gov/tio/download/remed/ss_sfund.pdf>.

[5] NSF. Contaminants in the subsurface: source zone assessment and remediation. Washington, DC: National Academies Press; 2004.

[6] Sale TC, McWhorter DB. Steady state mass transfer from single-component dense nonaqueous phase liquids in uniform flow fields. Water Resour Res 2001;37:393–404.

[7] Boparai HK, Joseph M, O'Carroll DM. Kinetics and thermodynamics of cadmium ion removal by adsorption onto nanozerovalent iron particles. J Hazard Mater 2011;186:458–65.

[8] Hwang YH, Kim DG, Shin HS. Mechanism study of nitrate reduction by nano zero valent iron. J Hazard Mater 2011;185:1513–21.

[9] Karabelli D, Üzüm Ç, Shahwan T, Eroğlu AE, Scott TB, Hallam KR, Lieberwirth I. Batch removal of aqueous Cu^{2+} ions using nanoparticles of zero-valent iron: A study of the capacity and mechanism of uptake. Ind Eng Chem Res 2008;47:4758–64.

[10] Li XQ, Cao JS, Zhang WX. Stoichiometry of Cr(VI) immobilization using nanoscale zerovalent iron (nZVI): a study with high-resolution X-ray photoelectron Spectroscopy (HR-XPS). Ind Eng Chem Res 2008;47:2131–9.

[11] Lien HL, Zhang WX. Nanoscale iron particles for complete reduction of chlorinated ethenes. Colloid Surface A 2001;191:97–105.

[12] Liu Y, Majetich SA, Tilton RD, Sholl DS, Lowry GV. TCE dechlorination rates, pathways, and efficiency of nanoscale iron particles with different properties. Environ Sci Technol 2005;39:1338–45.

[13] Liu ZG, Zhang FS. Nano-zerovalent iron contained porous carbons developed from waste biomass for the adsorption and dechlorination of PCBs. Bioresource Technol 2010;101:2562–4.

[14] Sarathy V, Salter AJ, Nurmi JT, Johnson GO, Johnson RL, Tratnyek PG. Degradation of 1,2,3-trichloropropane (TCP): hydrolysis, elimination, and reduction by iron and zinc. Environ Sci Technol 2010;44:787–93.

[15] Song H, Carraway ER. Reduction of chlorinated ethanes by nanosized zero-valent iron: kinetics, pathways, and effects of reaction conditions. Environ Sci Technol 2005;39:6237–45.

[16] He F, Zhao D. Preparation and characterization of a new class of starch-stabilized bimetallic nanoparticles for degradation of chlorinated hydrocarbons in water. Environ Sci Technol 2005;39:3314–20.

[17] He F, Zhao D. Manipulating the size and dispersibility of zerovalent iron nanoparticles by use of carboxymethyl cellulose stabilizers. Environ Sci Technol 2007;41:6216–21.

[18] He F, Zhao D, Paul C. Field assessment of carboxymethyl cellulose stabilized iron nanoparticles for in situ destruction of chlorinated solvents in source zones. Water Res 2010;44:2360–70.

[19] Phenrat T, Cihan A, Kim H-J, Mital M, Illangasekare T, Lowry GV. Transport and deposition of polymer-modified Fe^0 nanoparticles in 2-D heterogeneous porous media: Effects of particle concentration, Fe^0 content, and coatings. Environ Sci Technol 2010;44:9086–93.

[20] Phenrat T, Saleh N, Sirk K, Kim H-J, Tilton R, Lowry G. Stabilization of aqueous nanoscale zerovalent iron dispersions by anionic polyelectrolytes: adsorbed anionic polyelectrolyte layer properties and their effect on aggregation and sedimentation. J Nanopart Res 2008;10:795–814.

[21] Sakulchaicharoen N, O'Carroll DM, Herrera JE. Enhanced stability and dechlorination activity of pre-synthesis stabilized nanoscale FePd particles. J Contam Hydrol 2010;118:117–27.

[22] Saleh N, Phenrat T, Sirk K, Dufour B, Ok J, Sarbu T, et al. Adsorbed triblock copolymers deliver reactive iron nanoparticles to the oil/water interface. Nano Lett 2005;5:2489–94.

[23] Sun YP, Li XQ, Zhang WX, Wang HP. A method for the preparation of stable dispersion of zero-valent iron nanoparticles. Colloid Surface A 2007;308:60–6.

[24] Zhan JJ, Sunkara B, Le L, John VT, He JB, McPherson GL, et al. Multifunctional colloidal particles for in situ remediation of chlorinated hydrocarbons. Environ Sci Technol 2009;43:8616–21.

[25] Bennett P, He F, Zhao D, Aiken B, Feldman L. In situ testing of metallic iron nanoparticle mobility and reactivity in a shallow granular aquifer. J Contam Hydrol 2010;116:35–46.

[26] Quinn J, Geiger C, Clausen C, Brooks K, Coon C, O'Hara S, et al. Field demonstration of DNAPL dehalogenation using emulsified zero-valent iron. Environ Sci Technol 2005;39:1309–18.

[27] Elliott DW, Zhang W-x. Field assessment of nanoscale bimetallic particles for groundwater treatment. Environ Sci Technol 2001;35:4922–6.

[28] Zhang W-x. Nanoscale iron particles for environmental remediation: an overview. J Nanopart Res 2003;5:323–32.

[29] Wang C-B, Zhang W-X. Synthesizing nanoscale iron particles for rapid and complete dechlorination of TCE and PCBs. Environ Sci Technol 1997;31:2154–6.

[30] Sweeney KH, Fischer JR. Reductive degradation of halogenated pesticides. US Patent; 1972.

[31] Senzaki T, Kumagai Y. Removal of chlorinated organic compounds from waterwater by reduction process: treatment of 1,1,2,2-tetrachloroethane with iron powder. Kogyo Yosui 1988;357:2–7.

[32] Senzaki T, Kumagai Y. Removal of chlorinated organic compounds from waterwater by reduction process: treatment of trichloroethylene with iron powder. Kogyo Yosui 1989;369:19–25.

[33] Baciocchi R, Boni MR, D'Aprile L. Characterization and performance of granular iron as reactive media for TCE degradation by permeable reactive barriers. Water Air Soil Poll 2003;149:211–26.

[34] Gillham RW, O'Hannesin SF. Enhanced degradation of halogenated aliphatics by zero valent iron. Ground Water 1994;32:958–67.

[35] Orth WS, Gillham RW. Dechlorination of trichloroethene in aqueous solution using Fe–O. Environ Sci Technol 1996;30:66–71.

[36] Matheson LJ, Tratnyek PG. Reductive dehalogenation of chlorinated methanes by iron metal. Environ Sci Technol 1994;28. 2045-2045.

[37] Lien HL, Wilkin RT. High-level arsenite removal from groundwater by zero-valent iron. Chemosphere 2005;59:377.

[38] Blowes DW, Ptacek CJ, Benner SG, McRae CWT, Bennett TA, Puls RW. Treatment of inorganic contaminants using permeable reactive barriers. J Contam Hydrol 2000;45:123–37.

[39] Cantrell KJ, Kaplan DI, Wietsma TW. Zero-valent iron for the in-situ remediation of selected metals in groundwater. J Hazard Mater 1995;42:201–12.

[40] Gould JP. The kinetics of hexavalent chromium reduction by metallic iron. Water Res 1982;16:871–7.

[41] Moraci N, Calabro PS. Heavy metals removal and hydraulic performance in zero-valent iron/pumice permeable reactive barriers. J Environ Manage 2010;91:2336–41.

[42] Nikolaidis NP, Dobbs GM, Lackovic JA. Arsenic removal by zero-valent iron: field, laboratory and modeling studies. Water Res 2003;37:1417–25.

[43] Su CM, Puls RW. Arsenate and arsenite removal by zerovalent iron: kinetics, redox transformation, and implications for in situ groundwater remediation. Environ Sci Technol 2001;35:1487–92.

[44] Chuang FW, Larson RA, Wessman MS. Zero-valent iron-promoted dechlorination of polychlorinated-biphenyls. Environ Sci Technol 1995;29:2460–3.

[45] Wai CM, Yak HK, Wenclawiak BW, Cheng IF, Doyle JG. Reductive dechlorination of polychlorinated biphenyls by zerovalent iron in subcritical water. Environ Sci Technol 1999;33:1307–10.

[46] Waria M, Comfort SD, Onanong S, Satapanajaru T, Boparai H, Harris C, et al. Field-scale cleanup of atrazine and cyanazine contaminated soil with a combined chemical–biological approach. J Environ Qual 2009;38:1803–11.

[47] Satapanajaru T, Anurakpongsatorn P, Songsasen A, Boparai H, Park J. Using low-cost iron byproducts from automotive manufacturing to remediate DDT. Water Air Soil Poll 2006;175:361–74.

[48] Sayles GD, You GR, Wang MX, Kupferle MJ. DDT, DDD, and DDE dechlorination by zero-valent iron. Environ Sci Technol 1997;31:3448–54.

[49] Agrawal A, Tratnyek PG. Reduction of nitro aromatic compounds by zero-valent iron metal. Environ Sci Technol 1996;30:153–60.

[50] Bandstra JZ, Miehr R, Johnson RL, Tratnyek PG. Reduction of 2,4,6-trinitrotoluene by iron metal: kinetic controls on product distributions in batch experiments. Environ Sci Technol 2005;39:230–8.

[51] Hundal LS, Singh J, Bier EL, Shea PJ, Comfort SD, Powers WL. Removal of TNT and RDX from water and soil using iron metal. Environ Poll 1997;97:55–64.

[52] Cheng IF, Muftikian R, Fernando Q, Korte N. Reduction of nitrate to ammonia by zero-valent iron. Chemosphere 1997;35:2689–95.

[53] Young GK, Bungay HR, Brown LM, Parsons WA. Chemical reduction of nitrate in water. J Water Pollut Con Fed 1964;36:395–8.

[54] Arnold WA, Roberts AL. Pathways and kinetics of chlorinated ethylene and chlorinated acetylene reaction with Fe(0) particles. Environ Sci Technol 2000;34:1794–805.

[55] Tratnyek PG. Putting corrosion to use: remediating contaminated groundwater with zero-valent metals. Chem Ind (Lond) 1996:499.

[56] Johnson TL, Scherer MM, Tratnyek PG. Kinetics of halogenated organic compound degradation by iron metal. Environ Sci Technol 1996;30:2634–40.

[57] Gillham RW, Vogan J, Gui L, Duchene M, Son J. Iron barrier walls for chlorinated solvent remediation. In: Stroo HF, Ward CH, editors. In situ remediation of chlorinated solvent plumes. New York: Springer; 2010. p. 538.

[58] Wilkin RT, Su CM, Ford RG, Paul CJ. Chromium-removal processes during groundwater remediation by a zerovalent iron permeable reactive barrier. Environ Sci Technol 2005;39:4599–605.

[59] Henderson AD, Demond AH. Long-term performance of zero-valent iron permeable reactive barriers: a critical review. Environ Eng Sci 2007;24:401–23.

[60] Higgins MR, Olson TM. Life-cycle case study comparison of permeable reactive barrier versus pump-and-treat remediation. Environ Sci Technol 2009;43:9432–8.

[61] Phillips DH, Van Nooten T, Bastiaens L, Russell MI, Dickson K, Plant S, et al. Ten year performance evaluation of a field-scale zero-valent iron permeable reactive barrier installed to remediate trichloroethene contaminated groundwater. Environ Sci Technol 2010;44:3861–9.

[62] Li XQ, Elliot DW, Zhang Wx. Zero-valent iron nanoparticles for abatement of environmental pollutants: materials and engineering aspects. Crit Rev Solid State 2006;31:111–22.

[63] Nurmi JT, Tratnyek PG, Sarathy V, Baer DR, Amonette JE, Pecher K, et al. Characterization and properties of metallic iron nanoparticles: spectroscopy, electrochemistry, and kinetics. Environ Sci Technol 2005;39:1221–30.

[64] Rivero-Huguet M, Marshall WD. Reduction of hexavalent chromium mediated by micron- and nano-scale zero-valent metallic particles. J Environ Monit 2009;11:1072–9.

[65] Li XQ, Zhang WX. Sequestration of metal cations with zerovalent iron nanoparticles – a study with high resolution X-ray photoelectron spectroscopy (HR-XPS). J Phy Chem C 2007;111:6939–46.

[66] Barnes RJ, Riba O, Gardner MN, Scott TB, Jackman SA, Thompson IP. Optimization of nano-scale nickel/iron particles for the reduction of high concentration chlorinated aliphatic hydrocarbon solutions. Chemosphere 2010;79:448–54.

[67] Schrick B, Blough JL, Jones AD, Mallouk TE. Hydrodechlorination of trichloroethylene to hydrocarbons using bimetallic nickel–iron nanoparticles. Chem Mater 2002;14:5140–7.

[68] Sun YP, Li XQ, Cao JS, Zhang WX, Wang HP. Characterization of zero-valent iron nanoparticles. Adv Colloid Interface 2006;120:47–56.

[69] Uegami M, Kawano J, Okita T, Fujii Y, Okinaka K, Kakuyua K, et al. Iron particles for purifying contaminated soil or ground water. Process for producing the iron particles, purifying agent comprising the iron particles, process for producing the purifying agent and method of purifying contaminated soil or ground water. Toda Kogyo Corp., US Patent Application 2003/0217974 A1, 2003.

[70] Yoo BY, Hernandez SC, Koo B, Rheem Y, Myung NV. Electrochemically fabricated zero-valent iron, iron–nickel, and iron–palladium nanowires for environmental remediation applications. Water Sci Technol 2007;55: 149–56.

[71] Glavee GN, Klabunde KJ, Sorensen CM, Hadjipanayis GC. Chemistry of borohydride reduction of iron(II) and iron(III) ions in aqueous and nonaqueous media – formation of nanoscale Fe, Feb, and Fe_2 b powders. Inorg Chem 1995;34:28–35.

[72] Grinstaff MW, Salamon MB, Suslick KS. Magnetic-properties of amorphous iron. Phys Rev B 1993;48:269–73.

[73] Signorini L, Pasquini L, Savini L, Carboni R, Boscherini F, Bonetti E, et al. Size-dependent oxidation in iron/iron oxide core-shell nanoparticles. Phys Rev B 2003:68.

[74] Phenrat T, Saleh N, Sirk K, Tilton RD, Lowry GV. Aggregation and sedimentation of aqueous nanoscale zerovalent iron dispersions. Environ Sci Technol 2007;41:284–90.

[75] Liu Y, Choi H, Dionysiou D, Lowry GV. Trichloroethene hydrodechlorination in water by highly disordered monometallic nanoiron. Chem Mater 2005;17:5315–22.

[76] Phenrat T, Kim HJ, Fagerlund F, Illangasekare T, Tilton RD, Lowry GV. Particle size distribution, concentration, and magnetic attraction affect transport of polymer-modified Fe-0 nanoparticles in sand columns. Environ Sci Technol 2009;43:5079–85.

[77] Kakani SL, Kakani A. Material science. New Delhi: New Age International Publishers; 2004.

[78] Yan WL, Herzing AA, Kiely CJ, Zhang WX. Nanoscale zero-valent iron (nZVI): aspects of the core–shell structure and reactions with inorganic species in water. J Contam Hydrol 2010;118:96–104.

[79] Liu Y, Lowry GV. Effect of particle age (Fe^0 content) and solution pH on NZVI reactivity: H_2 evolution and TCE dechlorination. Environ Sci Technol 2006;40:6085–90.

[80] Bard AJ, Parsons R, Jordan J. Standard potentials in aqueous solution. Marcel Dekker, Inc.; 1985.

[81] Li T, Farrell J. Reductive dechlorination of trichloroethene and carbon tetrachloride using iron and palladized-iron cathodes. Environ Sci Technol 2000;34:173–9.

[82] Roberts AL, Totten LA, Arnold WA, Burris DR, Campbell TJ. Reductive elimination of chlorinated ethylenes by zero valent metals. Environ Sci Technol 1996;30:2654–9.

[83] Yu ZB, Qiao MH, Li HX, Deng JF. Preparation of amorphous Ni–Co–B alloys and the effect of cobalt on their hydrogenation activity. Appl Catal A – Gen 1997;163:1–13.

[84] Cook SM. Assessing the use and application of zero-valent iron nanoparticle technology for remediation at contamianted sites. Office of Solid Waste and Emergency Response, Office of Superfund Remediation and Technology Innovation; 2009.

[85] Su C, Puls RW. Kinetics of trichloroethene reduction by zerovalent iron and tin: pretreatment effect, apparent activation energy, and intermediate products. Environ Sci Technol 1999;33:163–8.

[86] Elsner M, Chartrand M, VanStone N, Lacrampe Couloume G, Sherwood Lollar B. Identifying abiotic chlorinated ethene degradation: characteristic isotope patterns in reaction products with nanoscale zero-valent iron; 2008. p. 5963–70.

[87] Mattes TE, Alexander AK, Coleman NV. Aerobic biodegradation of the chloroethenes: pathways, enzymes, ecology, and evolution. FEMS Microbiol Rev 2010;34:445–75.

[88] DiStefano TD, Gossett JM, Zinder SH. Reductive dechlorination of high concentrations of tetrachloroethene to ethene by an anaerobic enrichment culture in the absence of methanogenesis. Appl Environ Microbiol 1991;57:2287–92.

[89] He J, Ritalahti KM, Aiello MR, Loffler FE. Complete detoxification of vinyl chloride by an anaerobic enrichment culture and identification of the reductively dechlorinating population as a Dehalococcoides species. Appl Environ Microbiol 2003;69:996–1003.

[90] Isalou M, Sleep BE, Liss SN. Biodegradation of high concentrations of tetrachloroethene in a continuous flow column system. Environ Sci Technol 1998;32:3579–85.

[91] Hood ED, Major DW, Quinn JW, Yoon WS, Gavaskar A, Edwards EA. Demonstration of enhanced bioremediation in a TCE source area at Launch Complex 34, Cape Canaveral Air Force Station. Ground Water Monit Remed 2008;28:98–107.

[92] Morrill PL, Sleep BE, Seepersad DJ, McMaster ML, Hood ED, LeBron C, et al. Variations in expression of carbon isotope fractionation of chlorinated ethenes during biologically enhanced PCE dissolution close to a source zone. J Contam Hydrol 2009;110:60–71.

[93] Xiu Zm, Jin Zh, Li Tl, Mahendra S, Lowry GV, Alvarez PJJ. Effects of nano-scale zero-valent iron particles on a mixed culture dechlorinating trichloroethylene. Bioresource Technol 2010;101:1141–6.

[94] Xiu ZM, Gregory KB, Lowry GV, Alvarez PJJ. Effect of bare and coated nanoscale zerovalent iron on tceA and vcrA gene expression in Dehalococcoides spp. Environ Sci Technol 2010;44:7647–51.

[95] Alonso F, Beletskaya IP, Yus M. Metal-mediated reductive hydrodehalogenation of organic halides. Chem Rev 2002;102:4009–91.

[96] He F, Zhao DY. Hydrodechlorination of trichloroethene using stabilized Fe–Pd nanoparticles: reaction mechanism and effects of stabilizers, catalysts and reaction conditions. Appl Catal B – Environ 2008;84:533–40.

[97] Lien HL, Zhang WX. Nanoscale Pd/Fe bimetallic particles: catalytic effects of palladium on hydrodechlorination. Appl Catal B – Environ 2007;77:110–6.

[98] Lien H-L, Zhang W. Effect of palladium on the reductive dechlorination of chlorinated ethylenes with nanoscale Pd/Fe particles. Water Sci Technol 2004;4:297–303.

[99] Zhu BW, Lim TT. Catalytic reduction of chlorobenzenes with Pd/Fe nanoparticles: Reactive sites, catalyst stability, particle aging, and regeneration. Environ Sci Technol 2007;41:7523–9.

[100] Jacobs JA, Testa SM. Overview of chromium(VI) in the environment: background and history. In: Guertin J, Jacobs JA, Avakian CP, editors. Chromium(VI) handbook. New York: CRC Press; 2005. p. 1–21.

[101] Manning BA, Kiser JR, Kwon H, Kanel SR. Spectroscopic investigation of Cr(III)- and Cr(VI)-treated nanoscale zerovalent iron. Environ Sci Technol 2007;41:586–92.

[102] Ponder SM, Darab JG, Mallouk TE. Remediation of Cr(VI) and Pb(II) aqueous solutions using supported, nanoscale zero-valent iron. Environ Sci Technol 2000;34:2564–9.

[103] Hu CY, Lo SL, Liou YH, Hsu YW, Shih K, Lin CJ. Hexavalent chromium removal from near natural water by copper-iron bimetallic particles. Water Res 2010;44:3101–8.

[104] Rivero-Huguet M, Marshall WD. Reduction of hexavalent chromium mediated by micro- and nano-sized mixed metallic particles. J Hazard Mater 2009;169:1081–7.

[105] Korte NE, Fernando Q. A review of arsenic(III) in groundwater. Crit Rev Env Cont 1991;21:1–39.

[106] Ramos MAV, Yan W, Li XQ, Koel BE, Zhang WX. Simultaneous oxidation and reduction of arsenic by zero-valent iron nanoparticles: understanding the significance of the core–shell structure. J Phys Chem C 2009;113:14591–4.

[107] Kanel SR, Greneche J-M, Choi H. Arsenic(V) removal from groundwater using nano scale zero-valent iron as a colloidal reactive barrier material. Environ Sci Technol 2006;40:2045–50.

[108] Yan WL, Ramos MAV, Koel BE, Zhang WX. Multi-tiered distributions of arsenic in iron nanoparticles: Observation of dual redox functionality enabled by a core-shell structure. Chem Commun 2010;46:6995–7.

[109] Kanel SR, Manning B, Charlet L, Choi H. Removal of arsenic(III) from groundwater by nanoscale zero-valent iron. Environ Sci Technol 2005;39:1291–8.

[110] Kanel S, Nepal D, Manning B, Choi H. Transport of surface-modified iron nanoparticles in porous media and application to arsenic(III) remediation. J Nanopart Res 2007;9:725–35.

[111] Jegadeesan G, Mondal K, Lalvani SB. Arsenate remediation using nanosized modified zerovalent iron particles. Environ Prog 2005;24:289–96.

[112] Cao B, Ahmed B, Beyenal H. Immobilization of uranium in groundwater using biofilms. In: Shah V, editor. Emerging environmental technologies, vol. II. New York: Springer; 2010. p. 1–37.

[113] Yan S, Hua B, Bao ZY, Yang J, Liu CX, Deng BL. Uranium(VI) removal by nanoscale zerovalent iron in anoxic batch systems. Environ Sci Technol 2010;44:7783–9.

[114] Fiedor JN, Bostick WD, Jarabek RJ, Farrell J. Understanding the mechanism of uranium removal from groundwater by zero-valent iron using X-ray photoelectron spectroscopy. Environ Sci Technol 1998;32:1466–73.

[115] Crane RA, Dickinson M, Popescu IC, Scott TB. Magnetite and zero-valent iron nanoparticles for the remediation of uranium contaminated environmental water. Water Res 2011;45:2931–42.

[116] Dickinson M, Scott TB. The application of zero-valent iron nanoparticles for the remediation of a uranium-contaminated waste effluent. J Hazard Mater 2010;178:171–9.

[117] Riba O, Scott TB, Ragnarsdottir KV, Allen GC. Reaction mechanism of uranyl in the presence of zero-valent iron nanoparticles. Geochim Cosmochim Acta 2008;72:4047–57.

[118] Scheinost AC, Kirsch R, Banerjee D, Fernandez-Martinez A, Zaenker H, Funke H, et al. X-ray absorption and photoelectron spectroscopy investigation of

selenite reduction by Fe(II)-bearing minerals. J Contam Hydrol 2008;102:228–45.

[119] Mondal K, Jegadeesan G, Lalvani SB. Removal of selenate by Fe and NiFe nanosized particles. Ind Eng Chem Res 2004;43:4922–34.

[120] Olegario JT, Yee N, Miller M, Sczepaniak J, Manning B. Reduction of Se(VI) to Se(-II) by zerovalent iron nanoparticle suspensions. J Nanopart Res 2010;12:2057–68.

[121] Efecan N, Shahwan T, Eroglu AE, Lieberwirth I. Characterization of the uptake of aqueous Ni2+ ions on nanoparticles of zero-valent iron (nZVI). Desalination 2009;249:1048–54.

[122] Li XQ, Zhang WX. Iron nanoparticles: the core-shell structure and unique properties for Ni(II) sequestration. Langmuir 2006;22:4638–42.

[123] Xi YF, Mallavarapu M, Naidu R. Reduction and adsorption of Pb^{2+} in aqueous solution by nano-zero-valent iron – A SEM, TEM and XPS study. Mater Res Bull 2010;45:1361–7.

[124] Lien HL, Jhuo YS, Chen LH. Effect of heavy metals on dechlorination of carbon tetrachloride by iron nanoparticles. Environ Eng Sci 2007;24:21–30.

[125] Üzüm Ç, Shahwan T, Eroğlu AE, Hallam KR, Scott TB, Lieberwirth I. Synthesis and characterization of kaolinite-supported zero-valent iron nanoparticles and their application for the removal of aqueous Cu^{2+} and Co^{2+} ions. Appl Clay Sci 2009;43:172–81.

[126] Üzüm Ç, Shahwan T, Eroğlu AE, Lieberwirth I, Scott TB, Hallam KR. Application of zero-valent iron nanoparticles for the removal of aqueous Co^{2+} ions under various experimental conditions. Chem Eng J 2008;144:213–20.

[127] Celebi OC, Uzum T, Shahwan H, Erten N. A radiotracer study of the adsorption behavior of aqueous Ba^{2+} ions on nanoparticles of zero-valent iron. J Hazard Mater 2007;148:761–7.

[128] Liu P, Cai W, Li Z, Zeng H, Hu J. Optical study of the reduction of hexavalent chromium by iron-based nanoparticles. J Nanosci Nanotechnol 2010;10:5389–92.

[129] Zhu H, Jia Y, Wu X, Wang H. Removal of arsenic from water by supported nano zero-valent iron on activated carbon. J Hazard Mater 2009;172:1591–6.

[130] Liu QY, Bei YL, Zhou F. Removal of lead(II) from aqueous solution with amino-functionalized nanoscale zero-valent iron. Cent Eur J Chem 2009;7:79–82.

[131] Tratnyek PG, Johnson RL. Nanotechnologies for environmental cleanup. Nano Today 2006;1:44–8.

[132] Sarathy V, Tratnyek PG, Nurmi JT, Baer DR, Amonette JE, Chun CL, et al. Aging of iron nanoparticles in aqueous solution: effects on structure and reactivity. J Phys Chem C 2008;112:2286–93.

[133] Reinsch BC, Forsberg B, Penn RL, Kim CS, Lowry GV. Chemical transformations during aging of zerovalent iron nanoparticles in the presence of common groundwater dissolved constituents. Environ Sci Technol 2010;44:3455–61.

[134] Tamara ML, Butler EC. Effects of iron purity and groundwater characteristics on rates and products in the degradation of carbon tetrachloride by iron metal. Environ Sci Technol 2004;38:1866–76.

[135] Chen JL, Al-Abed SR, Ryan JA, Li ZB. Effects of pH on dechlorination of trichloroethylene by zero-valent iron. J Hazard Mater 2001;83:243–54.

[136] Phenrat T, Liu Y, Tilton RD, Lowry GV. Adsorbed polyelectrolyte coatings decrease Fe^0 nanoparticle reactivity with TCE in water: conceptual model and mechanisms. Environ Sci Technol 2009;43:1507–14.

[137] Lim TT, Zhu BW. Effects of anions on the kinetics and reactivity of nanoscale Pd/Fe in trichlorobenzene dechlorination. Chemosphere 2008;73:1471–7.

[138] Liu Y, Phenrat T, Lowry GV. Effect of TCE concentration and dissolved groundwater solutes on NZVI-promoted TCE dechlorination and H_2 evolution. Environ Sci Technol 2007;41:7881–7.

[139] Wang W, Zhou M, Jin Z, Li T. Reactivity characteristics of poly(methyl methacrylate) coated nanoscale iron particles for trichloroethylene remediation. J Hazard Mater 2010;173:724–30.

[140] Tee YH, Grulke E, Bhattacharyya D. Role of Ni/Fe nanoparticle composition on the degradation of trichloroethylene from water. Ind Eng Chem Res 2005;44:7062–70.

[141] Hoerle S, Mazaudier F, Dillmann P, Santarini G. Advances in understanding atmospheric corrosion of iron. II: Mechanistic modelling of wet–dry cycles. Corros Sci 2004;46:1431–65.

[142] Kim HS, Ahn JY, Hwang KY, Kim IK, Hwang I. Atmospherically stable nanoscale zero-valent iron particles formed under controlled air contact: characteristics and reactivity. Environ Sci Technol 2010;44:1760–6.

[143] Wang Q, Lee S, Choi H. Aging study on the structure of Fe(0)-nanoparticles: stabilization, characterization, and reactivity. J Phys Chem C 2010;114:2027–33.

[144] Sohn K, Kang SW, Ahn S, Woo M, Yang SK. Fe(0) nanoparticles for nitrate reduction: stability, reactivity, and transformation. Environ Sci Technol 2006;40:5514–9.

[145] Kim HS, Kang WH, Kim M, Park JY, Hwang I. Comparison of hematite/Fe(II) systems with cement/Fe(II) systems in reductively dechlorinating trichloroethylene. Chemosphere 2008;73:813–9.

[146] Boland DD, Collins RN, Payne TE, Waite TD. Effect of amorphous Fe(III) oxide transformation on the Fe(II)-mediated reduction of U(VI). Environ Sci Technol 2011;45:1327–33.

[147] Danielsen KM, Hayes KF. pH dependence of carbon tetrachloride reductive dechlorination by magnetite. Environ Sci Technol 2004;38:4745–52.

[148] Yan W, Herzing AA, Li XQ, Kiely CJ, Zhang WX. Structural evolution of Pd-doped nanoscale zero-valent iron (nZVI) in aqueous media and implications for particle aging and reactivity. Environ Sci Technol 2010;44:4288–94.

[149] Song H, Carraway ER. Reduction of chlorinated methanes by nano-sized zero-valent iron. Kinetics, pathways, and effect of reaction conditions. Environ Eng Sci 2006;23:272–84.

[150] Zhu NR, Luan HW, Yuan SH, Chen J, Wu XH, Wang LL. Effective dechlorination of HCB by nanoscale Cu/Fe particles. J Hazard Mater 2010;176:1101–5.

[151] Satapanajaru T, Anurakpongsatorn P, Pengthamkeerati P, Boparai H. Remediation of atrazine-contaminated soil and water by nano zerovalent iron. Water Air Soil Poll 2008;192:349–59.

[152] Freedman DL, Gossett JM. Biological reductive dechlorination of tetrachloroethylene and trichloroethylene to ethylene under methanogenic conditions. Appl Environ Microbiol 1989;55:2144–51.

[153] Liu CC, Tseng DH, Wang CY. Effects of ferrous ions on the reductive dechlorination of trichloroethylene by zero-valent iron. J Hazard Mater 2006;136:706–13.

[154] Bishop EJ, Fowler DE, Skluzacek JM, Seibel E, Mallouk TE. Anionic homopolymers efficiently target zerovalent iron particles to hydrophobic contaminants in sand columns. Environ Sci Technol 2010;44:9069–74.

[155] Zheng TH, Zhan JJ, He JB, Day C, Lu YF, Mcpherson GL, Piringer G, John VT. Reactivity characteristics of nanoscale zerovalent iron–silica composites for trichloroethylene remediation. Environ Sci Technol 2008;42:4494–9.

[156] Zhan J, Zheng T, Piringer G, Day C, McPherson GL, Lu Y, Papadopoulos K, John VT. Transport characteristics of nanoscale functional zerovalent iron/silica composites for in situ remediation of trichloroethylene. Environ Sci Technol 2008;42:8871–6.

[157] He F, Zhao D, Liu J, Roberts CB. Stabilization of Fe–Pd nanoparticles with sodium carboxymethyl cellulose for enhanced transport and dechlorination of trichloroethylene in soil and groundwater. Ind Eng Chem Res 2007;46:29–34.

[158] Schrick B, Hydutsky BW, Blough JL, Mallouk TE. Delivery vehicles for zerovalent metal nanoparticles in soil and groundwater. Chem Mater 2004;16:2187–93.

[159] Tiraferri A, Chen KL, Sethi R, Elimelech M. Reduced aggregation and sedimentation of zero-valent iron nanoparticles in the presence of guar gum. J Colloid Interface Sci 2008;324:71–9.

[160] Cirtiu CM, Raychoudhury T, Ghoshal S, Moores A. Systematic comparison of the size, surface characteristics and colloidal stability of zero valent iron nanoparticles pre- and post-grafted with common polymers. Colloid Surface A 2011;390:95–104.

[161] Huang Q, Shi X, Pinto RA, Petersen EJ, Weber WJ. Tunable synthesis and immobilization of zero-valent iron nanoparticles for environmental applications. Environ Sci Technol 2008;42:8884–9.

[162] Zhan JJ, Kolesnichenko I, Sunkara B, He JB, McPherson GL, Piringer G, John VT. Multifunctional iron–carbon nanocomposites through an aerosol-based process for the in situ remediation of chlorinated hydrocarbons. Environ Sci Technol 2011;45:1949–54.

[163] Xu J, Dozier A, Bhattacharyya D. Synthesis of nanoscale bimetallic particles in polyelectrolyte membrane matrix for reductive transformation of halogenated organic compounds. J Nanopart Res 2005;7:449–67.

[164] Kirschling TL, Gregory KB, Minkley EG, Lowry GV, Tilton RD. Impact of nanoscale zero valent iron on geochemistry and microbial populations in trichloroethylene contaminated aquifer materials. Environ Sci Technol 2010;44:3474–80.

[165] Wang Y, Zhou D, Wang Y, Zhu X, Jin S. Humic acid and metal ions accelerating the dechlorination of 4-chlorobiphenyl by nanoscale zero-valent iron. J Environ Sci 2011;23:1286–92.

[166] Kang S-H, Choi W. Oxidative degradation of organic compounds using zero-valent iron in the presence of natural organic matter serving as an electron shuttle. Environ Sci Technol 2009;43:878–83.

[167] Saleh N, Sirk K, Liu Y, Phenrat T, Dufour B, Matyjaszewski K, Tilton RD, Lowry GV. Surface modifications enhance nanoiron transport and NAPL targeting in saturated porous media. Environ Eng Sci 2007;24:45–57.

[168] Berge ND, Ramsburg CA. Iron-mediated trichloroethene reduction within nonaqueous phase liquid. J Contam Hydrol 2010;118:105–16.

[169] Taghavy A, Costanza J, Pennell KD, Abriola LM. Effectiveness of nanoscale zero-valent iron for treatment of a PCE-DNAPL source zone. J Contam Hydrol 2010;118:128–42.

[170] He F, Zhang M, Qian T, Zhao D. Transport of carboxymethyl cellulose stabilized iron nanoparticles in porous media: column experiments and modeling. J Colloid Interface Sci 2009;334:96–102.

[171] Lowry GV, Reinhard M. Pd-catalyzed TCE dechlorination in groundwater: solute effects, biological control, and oxidative catalyst regeneration. Environ Sci Technol 2000;34:3217–23.

[172] Farrell J, Kason M, Melitas N, Li T. Investigation of the long-term performance of zero-valent iron for reductive dechlorination of trichloroethylene. Environ Sci Technol 2000;34:514–21.

[173] Grittini C, Malcomson M, Fernando Q, Korte N. Rapid dechlorination of polychlorinated biphenyls on the surface of a Pd/Fe bimetallic system. Environ Sci Technol 1995;29:2898–900.

[174] Lowry GV, Reinhard M. Hydrodehalogenation of 1- to 3-carbon halogenated organic compounds in water using a palladium catalyst and hydrogen gas. Environ Sci Technol 1999;33:1905–10.

[175] Muftikian R, Nebesny K, Fernando Q, Korte N. X-ray photoelectron spectra of the palladium – iron bimetallic surface used for the rapid dechlorination of chlorinated organic environmental contaminants. Environ Sci Technol 1996;30:3593–6.

[176] Lien H-L, Zhang W-x. Transformation of chlorinated methanes by nanoscale iron particles. J Environ Eng – ASCE 1999;125:1042–7.

[177] Lien HL, Zhang WX. Hydrodechlorination of chlorinated ethanes by nanoscale Pd/Fe bimetallic particles. J Environ Eng – ASCE 2005;131:4–10.

[178] Hong YS, Honda RJ, Myung NV, Walker SL. Transport of iron-based nanoparticles: role of magnetic properties. Environ Sci Technol 2009;43:8834–9.

[179] Berge ND, Ramsburg CA. Oil-in-water emulsions for encapsulated delivery of reactive iron particles. Environ Sci Technol 2009;43:5060–6.

[180] Rosicka D, Sembera J. Assessment of influence of magnetic forces on aggregation of zero-valent iron nanoparticles. Nanoscale Res Lett 2011;6:10.

[181] Tiraferri A, Sethi R. Enhanced transport of zerovalent iron nanoparticles in saturated porous media by guar gum. J Nanopart Res 2009;11:635–45.

[182] Gavaskar ATL, Condit W. Contract report: cost and performance report: nanoscale zerovalent iron technologies for source remediation. NAVFAC: Naval Facilities Engineering Command; 2005.

[183] Krug T, O'Hara S, Watling M, Quinn J. Emulsified zero-valent nano-scale iron treatment of chlorinated solvent napl source zones. Geosyntec Consultants 2010.

[184] Wei YT, Wu SC, Chou CM, Che CH, Tsai SM, Lien HL. Influence of nanoscale zero-valent iron on geochemical properties of groundwater and vinyl chloride degradation: a field case study. Water Res 2010;44:131–40.

[185] Hydutsky BW, Mack EJ, Beckerman BB, Skluzacek JM, Mallouk TE. Optimization of nano- and microiron transport through sand columns using polyelectrolyte mixtures. Environ Sci Technol 2007;41:6418–24.

[186] Johnson RL, Johnson GO, Nurmi JT, Tratnyek PG. Natural organic matter enhanced mobility of nano zerovalent iron. Environ Sci Technol 2009;43:5455–60.

[187] Saleh N, Kim H-J, Phenrat T, Matyjaszewski K, Tilton RD, Lowry GV. Ionic strength and composition affect the mobility of surface-modified Fe^0 nanoparticles in water-saturated sand columns. Environ Sci Technol 2008;42:3349–55.

[188] Kim HJ, Phenrat T, Tilton RD, Lowry GV. Fe^0 nanoparticles remain mobile in porous media after aging due to slow desorption of polymeric surface modifiers. Environ Sci Technol 2009;43:3824–30.

[189] Cantrell KJ, Kaplan DI, Gilmore TJ. Injection of colloidal Fe^0 particles in sand with shear-thinning fluids. J Environ Eng – ASCE 1997;123:786–91.

[190] Comba S, Sethi R. Stabilization of highly concentrated suspensions of iron nanoparticles using shear-thinning gels of xanthan gum. Water Res 2009;43:3717–26.

[191] Vecchia ED, Luna M, Sethi R. Transport in porous media of highly concentrated iron micro- and nanoparticles in the presence of xanthan gum. Environ Sci Technol 2009.

[192] Hoch LB, Mack EJ, Hydutsky BW, Hershman JM, Skluzacek JM, Mallouk TE. Carbothermal synthesis of carbon-supported nanoscale zero-valent iron particles for the remediation of hexavalent chromium. Environ Sci Technol 2008;42:2600–5.

[193] Logan BE, Jewett DG, Arnold RG, Bouwer EJ, O'Melia CR. Clarification of clean-bed filtration models. J Environ Eng – ASCE 1995;121:869–73.

[194] Ryan JN, Elimelech M. Colloid mobilization and transport in groundwater. Colloid Surface A 1996;107:1–56.

[195] Tufenkji N, Elimelech M. Correlation equation for predicting single-collector efficiency in physicochemical filtration in saturated porous media. Environ Sci Technol 2004;38:529–36.

[196] Lecoanet HF, Bottero J-Y, Wiesner MR. Laboratory assessment of the mobility of nanomaterials in porous media. Environ Sci Technol 2004;38:5164–9.

[197] Li Y, Wang Y, Pennell KD, Abriola LM. Investigation of the transport and deposition of fullerene (C60) nanoparticles in quartz sands under varying flow conditions. Environ Sci Technol 2008;42:7174–80.

[198] Liu X, O'Carroll DM, Petersen EJ, Huang Q, Anderson CL. Mobility of multiwalled carbon nanotubes in porous media. Environ Sci Technol 2009;43:8153–8.

[199] Kretzschmar R, Robarge WP, Amoozegar A. Influence of natural organic matter on colloid transport through saprolite. Water Resour Res 1995;31:435–45.

[200] Varadhi SN, Gill H, Apoldo LJ, Blackman RA, Wittman WK. Full-scale nanoiron injection for treatment of groundwater contaminated with chlorinated hydrocarbons. In: Natural gas technologies conference; 2005.

[201] Bai R, Tien C. A new correlation for the initial filter coefficient under unfavorable surface interactions. J Colloid Interface Sci 1996;179:631–4.

[202] Tosco T, Sethi R. Transport of non-newtonian suspensions of highly concentrated micro- and nanoscale iron particles in porous media: a modeling approach. Environ Sci Technol 2010;44:9062–8.

[203] Raychoudhury T, Naja G, Ghoshal S. Assessment of transport of two polyelectrolyte-stabilized zero-valent iron nanoparticles in porous media. J Contam Hydrol 2011;118:143–51.

[204] Yao K-M, Habibian MT, O'Melia CR. Water and waste water filtration. Concepts and applications. Environ Sci Technol 1971;5:1105–12.

[205] Nelson KE, Ginn TR. New collector efficiency equation for colloid filtration in both natural and engineered flow conditions. Water Resour Res 2011:47.

[206] Baalousha M. Aggregation and disaggregation of iron oxide nanoparticles: influence of particle concentration, pH and natural organic matter. Sci Total Environ 2009;407:2093–101.

[207] Phenrat T, Kim HJ, Fagerlund F, Illangasekare T, Lowry GV. Empirical correlations to estimate agglomerate size and deposition during injection of a polyelectrolyte-modified Fe-0 nanoparticle at high particle concentration in saturated sand. J Contam Hydrol 2010;118:152–64.

[208] Chatterjee J, Gupta SK. An agglomeration-based model for colloid filtration. Environ Sci Technol 2009;43:3694.

[209] Kanel SR, Goswami RR, Clement TP, Barnett MO, Zhao D. Two dimensional transport characteristics of surface stabilized zero-valent iron nanoparticles in porous media. Environ Sci Technol 2008;42:896–900.

[210] Langevin CD, Guo W. MODFLOW/MT3DMS-based simulation of variable-density ground water flow and transport. Ground Water 2006;44:339–51.

[211] Henn KW, Waddill DW. Utilization of nanoscale zero-valent iron for source remediation—a case study. Remed J 2006:57–76.

[212] Otto M. Use of nanoscale zero-valent iron for site remediation. In: Balent I, editor. Field scale remediation experience using iron nanoparticles and evolving risk-benefit understanding; 2010. <http://www.clu-in.org/conf/tio/nano-iron_121410/prez/nano_ironbw.pdf>.

[213] Karn B, Kuiken T, Otto M. Nanotechnology and *in situ* remediation: a review of the benefits and potential risks. Environ Health Perspect 2009:117.

[214] Glazier R, Venkatakrishnan R, Gheorghiu F, Walata L, Nash R, Wei-xian Z. Nanotechnology takes root. Civil Eng 2003;73:64.

[215] Shi ZQ, Nurmi JT, Tratnyek PG. Effects of nano zero-valent iron on oxidation-reduction potential. Environ Sci Technol 2011;45:1586–92.

[216] PARS_Environmental. Pilot test final report: bimetalic nanoscale particle of groundwater at area 1; 2003.

[217] Simonet BM, Valcarcel M. Monitoring nanoparticles in the environment. Anal Bioanal Chem 2009;393:17–21.

[218] Mace C. Controlling groundwater VOCs: do nanoscale ZVI particles have any advantages over microscale ZVI of BNP. Pollut Eng 2006;38:24–8.

[219] De Wildeman S, Verstraete W. The quest for microbial reductive dechlorination of C-2 to C-4 chloroalkanes is warranted. Appl Microbiol Biotechnol 2003;61:94–102.